UCRL-50026-80-4

# LLNL Underground Coal Gasification Project Quarterly Progress Report— October through December 1980

Scientific Editor: D. U. Olness

General Editor: Wallace Clements

January 26, 1981

Lawrence Livermore National Laboratory

DISCLAIMER

This document was prepared as an account of work sponsored by an agency of the United States Government. Neither the United States Government nor the University of California nor any of their employees, makes any warranty, express or implied, or assumes any legal liability or responsibility for the accuracy, completeness, or usefulness of any information, apparatus, product, or process disclosed, or represents that its use would not infringe privately owned rights. Reference herein to any specific commercial products, process, or service by trade name, trademark, manufacturer, or otherwise, does not necessarily constitute or imply its endorsement, recommendation, or favoring by the United States Government or the University of California. The views and opinions of authors expressed herein do not necessarily state or reflect those of the United States Government thereof, and shall not be used for advertising or product endorsement purposes.

**Work performed under the auspices of the U.S. Department of Energy and the Gas Research Institute by the Lawrence Livermore National Laboratory under Contract W-7405-Eng-48.**

DISCLAIMER

This document was prepared as an account of work sponsored by an agency of the United States Government. Neither the United States Government nor the University of California nor any of their employees, makes any warranty, express or implied, or assumes any legal liability or responsibility for the accuracy, completeness, or usefulness of any information, apparatus, product, or process disclosed, or represents that its use would not infringe privately owned rights. Reference herein to any specific commercial product, process, or service by trade name, trademark, manufacturer, or otherwise, does not necessarily constitute or imply its endorsement, recommendation, or favoring by the United States Government or the University of California. The views and opinions of authors expressed herein do not necessarily state or reflect those of the United States Government or the University of California, and shall not be used for advertising or product endorsement purposes.

This report has been reproduced
directly from the best available copy.

Available to DOE and DOE contractors from the
Office of Scientific and Technical Information
P.O. Box 62, Oak Ridge, TN 37831
Prices available from (615) 576-8401, FTS 626-8401

Available to the public from the
National Technical Information Service
U.S. Department of Commerce
5285 Port Royal Rd.,
Springfield, VA 22161

Work performed under the auspices of the U.S. Department of Energy by Lawrence Livermore National Laboratory under Contract W-7405-ENG-48.

UCRL

**BEST AVAILABLE COPY**

**FOR ORIGINAL REPORT**

**CALL**

**REPORTS LIBRARY**

**X37097**

UCRL-50026-80-4
Distribution Category UC-90c

# LLNL Underground Coal Gasification Project Quarterly Progress Report— October through December 1980

Scientific Editor: D. U. Olness

General Editor: Wallace Clements

Manuscript date: January 26, 1981

LAWRENCE LIVERMORE LABORATORY
University of California • Livermore, California • 94550

Available from: National Technical Information Service • U.S. Department of Commerce
5285 Port Royal Road • Springfield, VA 22161 • $7.00 per copy • (Microfiche $3.50)

# CONTENTS

Summary . . . . . 1
Introduction . . . . . 1
Mathematical Modeling of Cavity Burn in Coal-Block Experiments . . . . . 2
    Mathematical Form of the Model . . . . . 6
    A Simple Example . . . . . 9
    Summary . . . . . 11
Plan for Cavity Burn Experiments in Large Coal Blocks . . . . . 12
    Description of the Experiment . . . . . 12
    Experimental Strategy . . . . . 15
    Component Systems . . . . . 17
    Future Tests . . . . . 18
Postburn Condition of UCG Process Wells . . . . . 20
    Coring the Collapsed Zone of Well P-1 at Hoe Creek No. 3 . . . . . 20
    Logging the Hanna II Process Wells . . . . . 20
Plan for Directionally Drilled Borehole for the DOE Experiment No. 1 with WIDCO in Washington . . . . . 22
    Drilling Equipment . . . . . 22
    Drilling Program . . . . . 23
Analysis of Burn Cavity Growth in Hoe Creek No. 3 . . . . . 25
Groundwater Contamination Measurements at Hoe Creek No. 2 . . . . . 36
    Pregasification Results . . . . . 37
    Results During Gasification . . . . . 39
    Postgasification Results . . . . . 42
References . . . . . 52

# LLNL Underground Coal Gasification Project Quarterly Progress Report— October through December 1980

## SUMMARY

We have continued our laboratory studies of forward gasification through drilled holes in small blocks of coal (approximately 30 cm on a side). Such studies give insight into cavity growth mechanisms and particulate production. In addition, we have been developing a mathematical model for these experiments in order to further our understanding of the physical and chemical processes governing the burning of the coal and the growth of the cavity within the block. This model will be adapted, later, to larger-scale coal-block experiments, and finally to full-scale field experiments. We hope to obtain scaling laws and other insights from the model.

The small-block experiments are beginning to provide information relevant to the early-time cavity growth. The natural extension of these experiments to larger blocks, perhaps 10 ft or more on a side, is presently being planned. The large-block tests will be conducted at a mine, where blocks of coal will be isolated by the experimenter; the objective will be to quantify early-time cavity growth.

During this quarter we completed the planning for the directionally drilled injection well for DOE Experiment No. 1, to be carried out jointly by LLNL and the Washington Irrigation and Development Co. (WIDCO) near Centralia, Washington.

Assessment of the data obtained during the various underground coal gasification tests is continuing. Results from the four different diagnostic systems have been combined to produce a description of the shape of the burn cavity as a function of time during the Hoe Creek No. 3 experiment.

Groundwater samples from wells located at distances of a few feet to several hundred feet from the gasification cavities have been collected before, during, and after each of the Hoe Creek tests. During this quarter, the analysis of the groundwater contamination data pertinent to the Hoe Creek No. 2 test was completed.

## INTRODUCTION

A major objective of the U.S. Energy Program is to develop environmentally acceptable and economically sound ways to produce energy from the nation's vast coal reserves. The Department of Energy (DOE) has sponsored a number of field projects to determine the feasibility of converting coal into a clean, efficient energy source by underground coal gasification (UCG). The basic goal of the LLNL project, as a part of DOE's UCG program, is to develop a process for producing medium-heating-value gas that can be economically upgraded to pipeline quality gas or used to produce transportation fuels such as methanol or gasoline.

For the UCG process to function effectively in a coal seam, flow channels through the coal must exist, or be created, to provide adequate circulation between the injection and production wells. Our first two field experiments were designed to test two different techniques for creating such flow channels: (1) explosive fracturing of the coal in the seam, in

Hoe Creek No. 1, and (2) reverse burning, to enlarge existing passages through the coal, in Hoe Creek No. 2. For reasons of economy, both these experiments injected air to support the combustion.

Hoe Creek No. 3 was the world's first long-term UCG experiment in which a steam-oxygen mixture was injected, and the first in the United States to use a (horizontal) drilled hole within the coal seam to connect the injection and production wells.

The three Hoe Creek tests were conducted at shallow depths to maximize information and minimize expenses. We now plan to work at a deeper coal site (500 feet or deeper) because such deposits are the target resources for the underground coal conversion technology. In choosing the deeper test site we will look for one with a more favorable geological setting than at Hoe Creek—that is, one with stronger and dryer rock above the coal. By comparing the results from the deep test with those from the Hoe Creek tests, we will learn more about the effects of the surrounding rocks on the process.

# MATHEMATICAL MODELING OF CAVITY BURN IN COAL-BLOCK EXPERIMENTS

We have been developing a mathematical model for the laboratory-scale coal block experiments in order to better understand the physical and chemical processes governing the growth of the burn cavity within the block. The model will later be adapted to larger-scale coal block experiments, and finally to full-scale field experiments. We hope to obtain scaling laws and other insights from the model.

Figure 1 is a schematic view of a small coal-block experiment. In similar, somewhat larger experiments, a hole approximately 1 cm in diameter is drilled lengthwise through a block of coal cut to fit in a 55-gallon drum; the hole is approximately 1 meter long, and is surrounded by coal out to a distance of about 30 cm.

We are still developing our model; the work reported here consists of a definition of the major physical and chemical processes which seem to govern the growth of the burn cavity in the block. Our description is not novel. We use a small set of conventional physical submodels which we have selected as relevant from a much larger set of possible submodels.

For example, there are numerous models of coal gasification based on a packed-bed reactor (Table 1) that do not seem applicable. In the packed-bed reactor there is a forced flow of air through the bed which dominates the fluid flow. whereas in our block experiments the principal gas flow is parallel to the surface of the coal, and the dominant gas flow within the coal is the flow of water vapor and volatiles out of the bulk coal into the gas stream. This flow is at low velocity, roughly three orders of magnitude lower than flow velocities in the borehole.

Nevertheless, several existing numerical models (Table 2) are applicable to our situation. What follows is a summary of the physical submodels required, along with a steady-state approximation which reduces the problem of heat and mass flow in the coal from a partial differential equation to a set of algebraic equations.

In the experiments, air or a mixture of oxygen and steam flows through the borehole at a rate of about 0.1 mole/s, resulting in a velocity of about 20 m/s. This is sufficient to make the flow turbulent, even if the feed flow were laminar, which it is not. Because we wish to model an experiment which lasts for hours, we will treat the flow in the borehole as steady, turbulent flow with a boundary layer. For purposes of analysis we will divide the coal block and borehole into a number of washer-shaped zones, sliced perpendicular to the bore. A wedge-shaped segment of such a zone is shown schematically in Fig. 2, along with the temperature profile. Mass and energy will be transported through the boundary layer. Upstream, the gas will be cool and relatively rich in oxygen. If the surface of the coal is hot enough to support oxidation reactions, oxygen will be transported from the gas to the surface, and reaction products in the opposite direction. Heat will also be transferred from the surface to the gas. Downstream, the gas will be depleted in oxygen, but rich in reaction products. It may also be heated above the temperature of the coal surface at

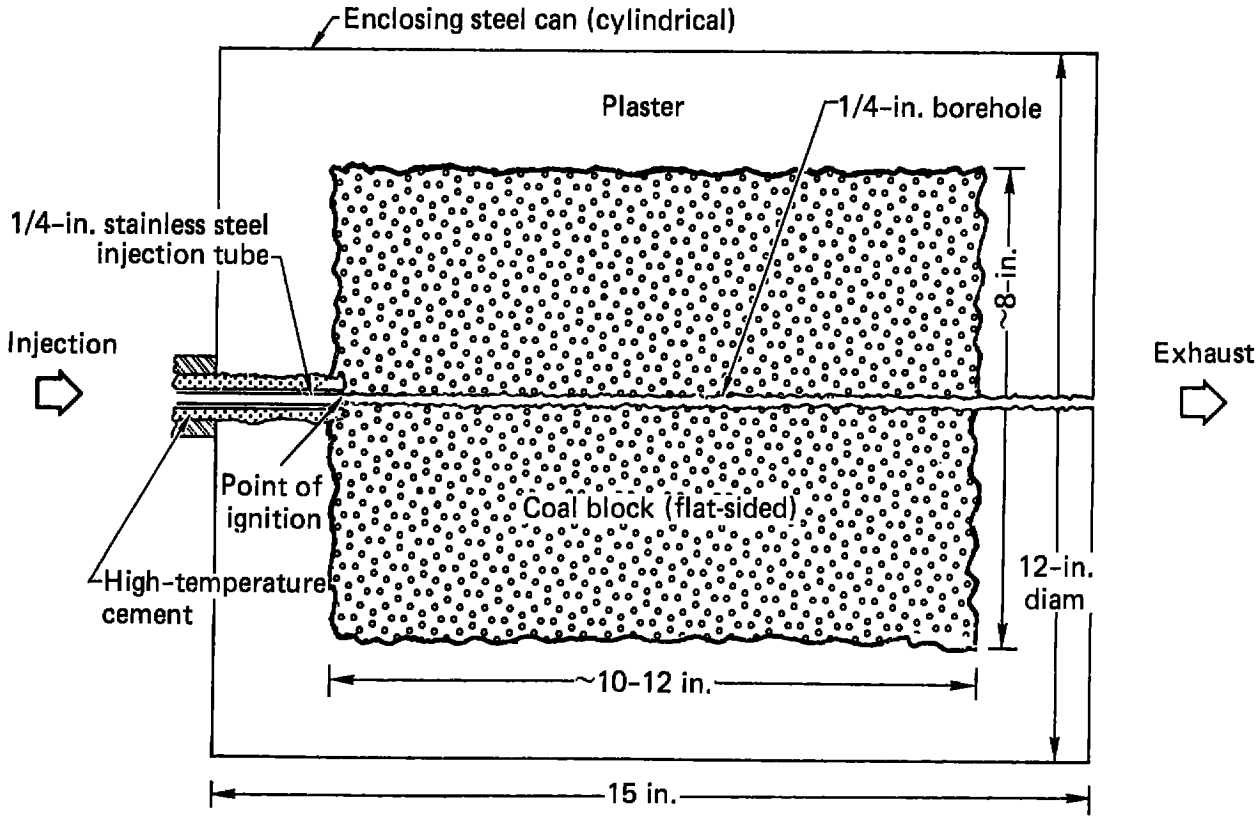


**FIG. 1. Experimental setup for borehole combustion tests in coal blocks (axial cross section through reactor).**

**TABLE 1. A few of the many numerical models that have been developed for coal gasification in a packed-bed reactor. These models are not applicable to cavity burn experiments in coal blocks, which are of interest here.**


Campbell, J. H., *Preliminary Modeling of Roof Collapse and Calculation of Gas Loss, Water Influx, and Surface Subsidence Associated with the Packed-Bed Scheme of In Situ Coal Gasification*, Lawrence Livermore National Laboratory, Livermore, Calif., UCID-16817 (1975).

Galil, R. D., G. E. Jones, and F. E. Kiviat, "Method for Evaluating the Significance of Observed Variations in Underground Coal Gasification," *Proc. Sixth Underground Coal Conversion Symposium* (Shangri-La, near Afton, Oklahoma, July 13–17, 1980), CONF-800716 (1980), p. III-56. Available from National Technical Information Service.

Gunn, R. D., D. L. Whitman, and D. D. Fischer, "A Permeation Theory for In Situ Coal Gasification," *Soc. Petrol. Eng. J.*, 300 (Oct. 1978).

Jennings, J. W., R. F. Strickland, and W. D. Von Gonten, "Texas A&M Project Status: Underground Lignite Gasification," *Proc. Third Annual Underground Coal Conversion Symposium* (Fallen Leaf Lake, California, June 6–9, 1977), CONF-770652 (1977), p. 83.

Krantz, W. B., D. W. Camp, and R. D. Gunn, "A Water-Influx Model for UCG," *Proc. Sixth Underground Coal Conversion Symposium*, CONF-800716 (1980), p. III-21.

Krauss, U., and B. Marzilger, "Numerical Simulation of an In Situ Filtration Gasification Process," *Proc. Sixth Underground Coal Conversion Symposium*, CONF-800716 (1980), P. III-32.

Thorsness, C. B., and C. J. Cena, "In Situ Coal Gasification Modeling," presented at AIChE Meeting, Houston, Texas, April 1979. See also Lawrence Livermore National Laboratory, Livermore, Calif., UCRL-82269 Preprint (Feb. 2, 1979).

Thorsness, C. B., and R. B. Rozsa, "In Situ Coal Gasification: Model Calculations and Laboratory Experiments," *Soc. Petrol. Eng. J.*, 105 (April 1978).

Winslow, A. M., "Numerical Model of Coal Gasification in a Packed Bed," *Proc. 16th Symposium on Combustion* (MIT, Cambridge, Mass., 1976), p. 503. See also Lawrence Livermore National Laboratory, Livermore, Calif., UCRL-77627 Preprint (April 1976).

**TABLE 2. Some existing numerical models that are applicable to the coal-block cavity burn experiments being done at LLNL.**

| |
|---|
| Dinsmoor, B., J. M. Galland, and T. F. Edgar, "The Modelling of Channel Formation During Underground Coal Gasification," *J. Petrol.*, 695 (May 1978). |
| Gibson, M. A., R. E. Pennington, and J. A. Wheeler, "Mathematical Modeling of Linked Vertical Well In Situ Coal Gasification," *Proc. Sixth Underground Coal Conversion Symposium*, CONF-800716 (1980), p. III-1. |
| Kashiwa, B. A., and F. H. Harlow, "Hot Gas Drying Calculations for a Coal Seam Channel," *Proc. Sixth Underground Coal Conversion Symposium*, CONF-800716 (1980), p. III-65. |
| Pasha, M. L., and S. M. Faroug Ali, "An Advanced Numerical Model of Underground Coal Gasification by the Stream Method, Using Simultaneous Solution," *Soc. Petrol. Eng. AIME*, SPE-7416 (1978). |
| Riggs, J. B., T. F. Edgar, and C. M. Johnson, "Development of a Three-Dimensional Simulator for Cavity Growth During Underground Coal Gasification," *Proc. Fifth Underground Coal Conversion Symposium*, CONF-790630 (1979), p. 245. |
| Schwartz, S. H., T. L. Eddy, and G. E. Nielsson, "A Simple UCG Cavity Model with Complex Energy Balance," *Proc. Sixth Underground Coal Conversion Symposium*, CONF-800716 (1980), p. III-69. |

that location, and heat will then be transferred from the gas to the coal. Thus the gas stream provides coupling between the washer-shaped zones of coal. Additional coupling between zones will be provided by thermal radiation. Because these couplings are expected to be large, and gradients in the solid parallel to the flow are expected to be small, longitudinal transport in the solid will be neglected.

We will now concentrate on the heat and mass flows in a single zone. These are shown schematically in Fig. 3. In Figs. 2 and 3 the surface of the coal is assumed hot enough to support oxidation reactions, which provide the heat to be transferred. These reactions also consume char, as do the anoxic reactions, so the surface of the coal is moving to the right at some velocity v. In that case the temperature profile assumes a steady state in a coordinate frame moving at velocity v. The various fronts then move together and the mass of char and dried coal remains constant, along with the heat stored in those zones. (This is discussed in more mathematical detail below.)

Because we are in a moving frame, wet coal is fed into the system on the right-hand side. It is then dried, releasing steam at a rate equal to the density of water in the wet coal multiplied by the velocity v, with roughly a thousandfold increase in volume. Because we have assumed steady state, this vapor cannot accumulate and must flow to the left.

(It could also flow to the right, where it would condense and give up its heat. In a coal which shrinks upon drying, it seems more likely that the vapor would flow out toward the borehole. The opposite might be true in a coal which expands upon drying. The model can be modified to handle either case if the fractions of flow in the two directions can be estimated. Water influx in field experiments can also be treated.)

The heat required to vaporize the water is normally much larger than that required to heat the (wet) coal; but both are proportional to the mass crossing the drying front, so the heat flux is proportional to the velocity. The heat flux is also proportional to the temperature gradient, so there are discontinuities in the slope of the temperature profile at each front in Fig. 2.

As we move toward the borehole the temperature rises until volatiles are driven off from the coal. This process is usually endothermic, and the mass flux of volatiles, as well as the heat flux, is again proportional to the velocity. At still higher temperatures the steam begins to react with the char, and other reactions of the volatiles may occur. If these reactions occur at some distance from the coal surface, there will be no oxygen present because it is all consumed at the surface. Therefore this reaction zone has been labeled "anoxic reaction" in the figures. If the surface temperature is high enough the anoxic reaction products will be determined by thermodynamic equilibrium. At lower surface temperatures the reaction rate will probably be limited by chemical kinetic rates, because the activation energy for the steam-char reaction is greater than that for the oxygen-char

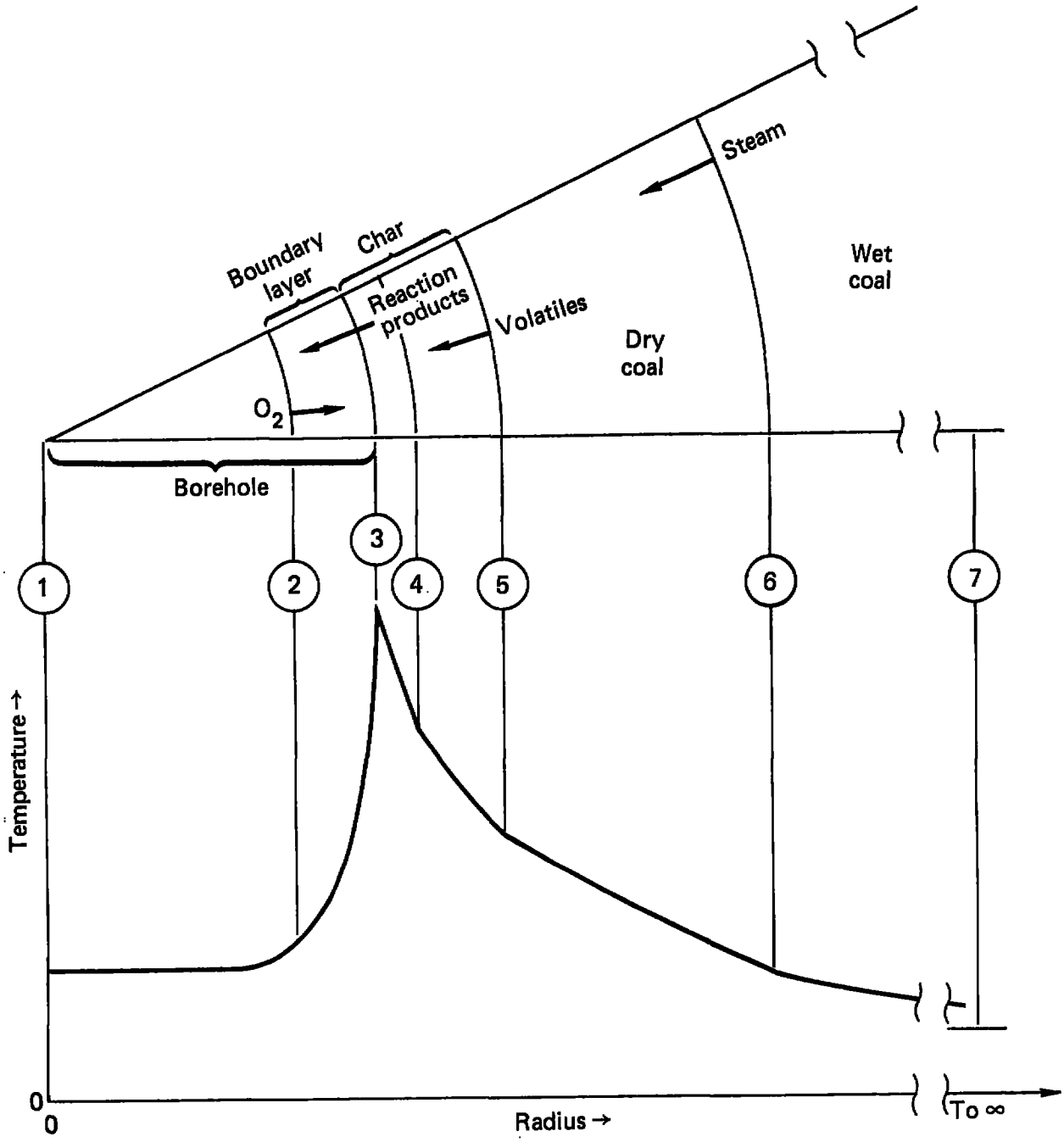


Legend

1. Centerline of borehole.
2. Edge of boundary layer.
3. Coal face and oxidation front.
4. Anoxic reaction front.
5. Volatilization front.
6. Drying front.
7. Virgin coal.

**FIG. 2. Wedge section of a transverse slice of the coal block during a cavity burn experiment, showing temperature vs radius for the various reaction regions involved. The block is divided into a number of such slices or zones for analysis.**

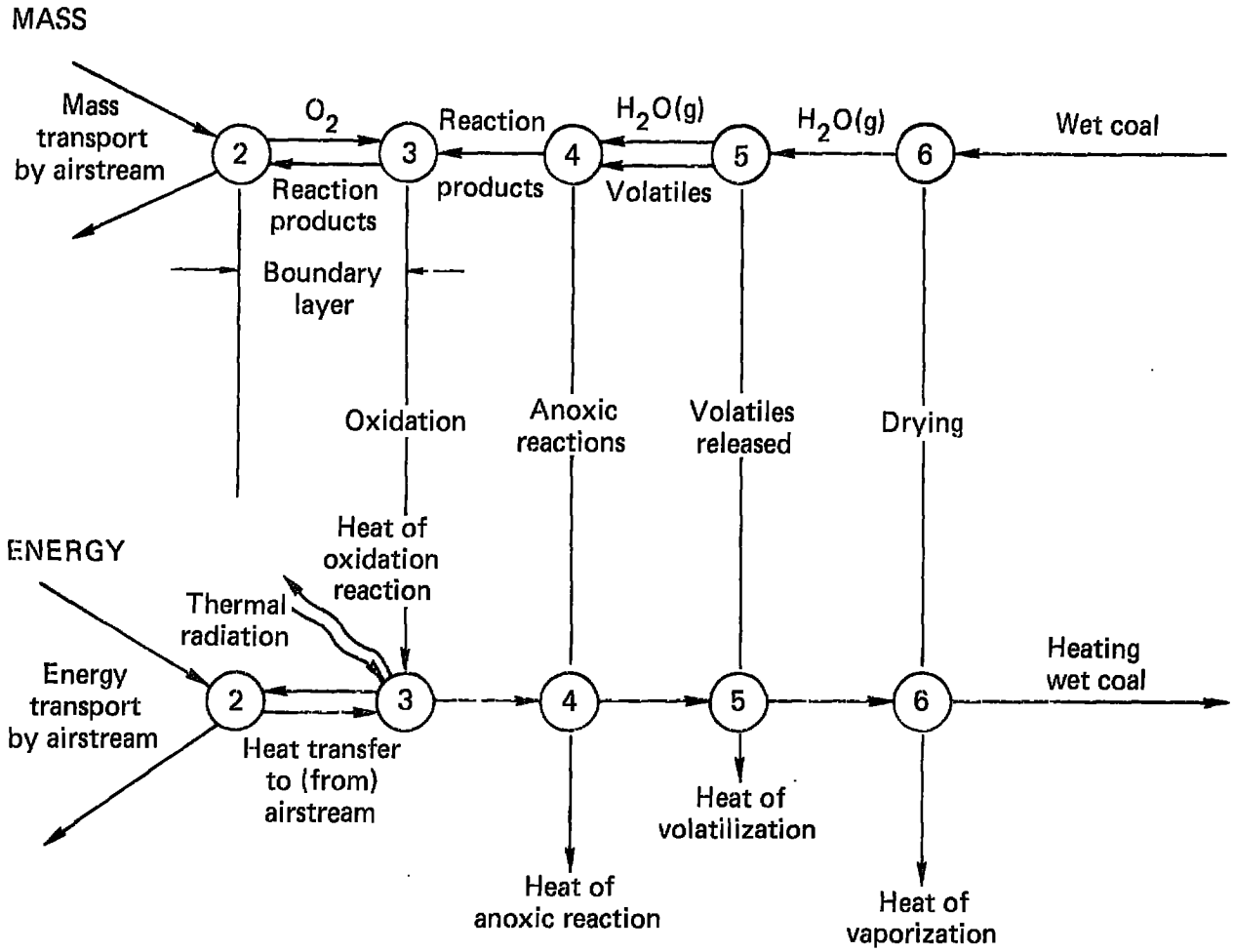


**FIG. 3. Radial mass and energy flow in a typical zone of the coal block. Circled numbers refer to the region boundaries defined in Fig. 2.**

reaction. This will also cause the two reaction zones to coalesce into one zone. Even when the steam-char reaction rate is kinetically limited, some reactions such as the water-gas-shift reaction are likely to be in thermodynamic equilibrium. When the surface temperature is sufficiently low, the anoxic reactions can be neglected entirely.

If the surface temperature is sufficient the char will be oxidized at the surface. The rate at which oxygen can be transported through the boundary layer is limited, setting an upper limit on the oxidation rate. At lower temperatures the oxidation rate may be kinetically limited, and at sufficiently low temperatures it will be negligible. The gas stream may contain water, so the steam-char reaction may occur at the surface, as well as at the anoxic reaction front. In addition, some of the volatiles may react with oxygen and reduce the rate of char consumption if the reaction rate is limited by oxygen transport.

The velocity at which the coal surface recedes is determined by the rate at which carbon is consumed. The other processes have rates proportional to this velocity, so logically we have completed the picture except that the heat balance may be affected by heat lost through radiation or gained by radiation from hotter zones. The ash found in coal has been neglected. It is easiest, but not necessary, to assume it flakes off as the char is consumed.

## MATHEMATICAL FORM OF THE MODEL

The verbal description of a single zone will now be translated into mathematical formulas.

The first step is to obtain a mathematical description of the mass transfer through the boundary layer. Mass transfer can be handled in the same

manner as the heat transfer, allowing us to use established recipes for heat transfer coefficients to calculate the mass transfer. The rate of heat flow per unit area, $\dot{q}$, through the boundary layer is given by

$$\dot{q} = h(T_g - T_s), \tag{1}$$

where h is the heat transfer coefficient, and $T_g$ and $T_s$ are the temperatures in the gas stream and at the surface. This can be rewritten in the form

$$\dot{q} = (h/C)(H_g - H_s), \tag{2}$$

where C is the appropriate specific heat of the gas, and $H_g$ and $H_s$ are the enthalpies of the gas in the stream and at the coal surface. The Reynolds analogy states that in a turbulent flow the rates of heat and mass transfer are proportional because both are transported by the same motions. Less restrictive assumptions lead to the same result,[1,2] so that the mass transport per unit area of species i, $m_i$, is given by

$$m_i = gB_i, \tag{3}$$

where $B_i$ is a mass transport potential analogous to the enthalpy difference in Eq. (2). $B_i$ is generally proportional to a concentration or mass fraction difference, and g (when it is expressed in the correct units) is numerically equal to h/C from Eq. (2). The appropriate forms for $B_i$ under different conditions can be found in Kays,[2] and the value of g can be estimated by methods established for calculating h. So the problem of calculating mass transfer from the gas to the coal surface is reduced to a simple analogy with the heat transfer.

The second step is to establish a formula for the transport of heat through the solid. This is governed by the diffusion equation, which in one-dimensional Cartesian coordinates is

$$\alpha\, \partial^2 T/\partial x^2 = \partial T/\partial t, \tag{4}$$

with

$$\alpha = k/\rho C,$$

where k is the thermal conductivity, $\rho$ the density, and C the specific heat of the material in question. The parameter $\alpha$ is a property of the material and is called the thermal diffusivity. Most solutions of Eq. (4) give complex formulas for T, with dependence on both x and t. A simple solution can be obtained for the case where the source of heat is moving at a constant velocity, v. The transformation $\xi = x - vt$ transforms the time derivative to a spatial derivative, and Eq. (4) reduces to an ordinary differential equation,[1]

$$d^2T/d\xi^2 + (v/\alpha)dT/d\xi = 0, \tag{5}$$

with a general solution

$$T = c_1 + c_2 e^{-v\xi/\alpha}. \tag{6}$$

The constants are determined by the boundary conditions. Referring to Fig. 2, we note that all temperatures are known except $T_3$ at the surface of the coal. If we treat $T_3$ as an independent variable, the appropriate boundary conditions in the solid are that the temperature is known at both ends of every interval in space. When the temperature is $T_0$ at $\xi_0$ and $T_1$ at $\xi_1$, then

$$\frac{T - T_0}{T_1 - T_0} = 1 - \frac{1 - \exp[-v(\xi - \xi_0)/\alpha]}{1 - \exp[-v(\xi_1 - \xi_0)/\alpha]}. \tag{7}$$

We can fit these segments together using the energy balance, which is shown schematically in Fig. 3. The heat flux at any point, $\xi$, in a segment is given by

$$\dot{q}(\xi) = -k\, dT(\xi)/d\xi. \tag{8}$$

Differentiating and rearranging Eq. (7) gives

$$\frac{\dot{q}(\xi)}{v\rho C(T_1 - T_0)} = \frac{\exp[-v(\xi - \xi_0)/\alpha]}{1 - \exp[-v(\xi_1 - \xi_0)/\alpha]}. \tag{9}$$

If we consider the interval from $\xi_n$ to $\xi_{n+1}$, we can define a function

$$E_n(\xi_n, \xi_{n+1}, v, \alpha) = \exp[-v(\xi_n - \xi_{n+1})/\alpha]. \tag{10}$$

Substituting this in Eq. (9) gives, at the boundaries,

$$\begin{aligned} \dot{q}_n(\xi_n) &= v\rho_n C_n(T_n - T_{n+1})/(1 - E_n), \\ \dot{q}_n(\xi_{n+1}) &= E_n\, \dot{q}_n(\xi_n), \end{aligned} \tag{11}$$

where the n subscript means that quantities are defined inside the interval, except for temperature which is defined at the endpoints. Note that $\dot{q}_n(\xi_{n+1})$ does not equal $\dot{q}_{n+1}(\xi_{n+1})$, but differs from it by the amount of heat that goes into the process assumed to be occurring at node n + 1: for example, drying. This difference gives us a further set of equations.

$$\dot{q}_6(\xi_6) = v\rho_6 C_6(T_6 - T_7),$$

$$\dot{q}_5(\xi_6) = \dot{q}_6(\xi_6) + v\rho_w \Delta H_{vap},$$

$$\dot{q}_4(\xi_5) = \dot{q}_5(\xi_5) + v\rho_{vol}\Delta H_{vol}, \qquad (12)$$

$$\dot{q}_3(\xi_4) = \dot{q}_4(\xi_4) + v(\rho_{vol} + \rho_{vap})\Delta H_{ar},$$

$$\dot{q}_3(\xi_3) = h(T_2 - T_3) + gB_{O_2}\Delta H_{or} + \dot{q}_{rad},$$

where $\rho_w$ is the density of water in the wet coal, $\rho_{vol}$ is the density of volatiles in the dry coal, $\Delta H_{vap}$ and $\Delta H_{vol}$ are the heats of vaporization and volatilization, $\Delta H_{ar}$ and $\Delta H_{or}$ are the heats of the anoxic and oxidation reactions per unit mass of mixture of steam and volatiles, and $\dot{q}_{rad}$ is the net energy gain at the coal surface due to radiative heat transfer. The radiative heat transfer will depend on the temperature and location of other surfaces within view of the coal surface of the current zone. If the optical view factor to the surface k at absolute temperature $T_k$ is $f_k$, the radiative heat transfer depends on the sum of all such visible surfaces, i.e., surfaces with $f_k$ nonzero.

$$\dot{q}_{rad} = \sigma\left(-T_3^4 + \sum f_k T_k^4\right), \qquad (13)$$

where $\sigma$ is the Stefan-Boltzmann constant. The form chosen for the heat release by the oxidation reaction, $gB_{O_2}\Delta H_{or}$, assumes that the reaction rate is limited by the rate of oxygen transfer across the boundary. Similarly, it is assumed that the anoxic reaction rate is limited by the availability of steam and volatiles.

Equations (11) through (13) form a system which can be solved for the various $E_n$'s. The velocity, v, is determined by the rate of char consumption. For example, if $\eta$ grams of char are consumed by the oxidation reaction for every gram of oxygen, and $\zeta$ moles of char per gram of steam and volatiles are consumed in the anoxic reactions, then

$$v = \eta g B_{O_2}/\rho_{char} + \zeta(\rho_w + \rho_{vol})/\rho_{char}. \qquad (14)$$

Once v and the values of the $E_n$'s are known, the $\xi_n$'s can be determined and we have an algebraic solution for the heat and mass flow in the solid.

The functions $E_n$ were defined in Eq. (10) in terms of an exponential. This is the solution of the diffusion equation in Cartesian coordinates; in cylindrical coordinates $E_n$ would have to be expressed in terms of Bessel functions. This change would not affect the validity of the algebraic solution. Indeed, the only restriction on the $E_n$'s is that they depend only on $\xi_n$, $\xi_{n+1}$, v, and $\alpha$. This is also relevant to the assumption that processes such as release of volatiles occur at a discrete temperature and location. If they are in fact spread out over some interval, the appropriate $E_n$ could be modified to account for this.

The form of Eqs. (12) gives the appearance that the algebraic problem is linear, or nearly so. It will generally be nonlinear, with the nonlinearities concealed in the radiation term, the heats of reaction, and the mass and heat transfer to the gas stream, the properties of which are perturbed by what happens in the solid. In fact, calculating the heat of reaction might involve solving one or more ordinary differential equations if the rate is kinetically limited. We are currently determining the proper form for these functions. However, the same calculations, or more complex ones, would be required to solve the partial differential equation. Reducing it in a rigorous way to an algebraic equation is a true simplification of the problem.

The algebraic solution depends on the assumption that a steady-state solution exists. Is this a valid assumption? Clearly, if v is large enough it can catch up with any fronts whose motion is driven by heat transfer from the surface. We can make some numerical estimates to see if this is applicable to the experiments we wish to model. From experimental data we find that at high surface temperatures v is on the order of $10^{-3}$ cm/s. From tabulated material properties we find that $\alpha$ is about $10^{-3}$ cm$^2$/s, so the drying front will be about a centimeter from the surface of the coal. We can estimate the time it would take heat to penetrate to a depth of 1 cm if v were zero. Solutions of the diffusion equation when v is

zero are complex, but the leading term in the solution can be approximated:

$$T(x)/T_{surface} \approx e^{-x^2/4\alpha t}.$$

At some distance x the time constant for temperature rise will be $\tau = x^2/4\alpha$. At the approximate depth of the drying front, x is $\alpha/v$ and the time constant is $\alpha/(4v^2)$. When v is 0.001 cm/s the time constant will be about 250 s, or 4 minutes, sufficiently short for our modeling purposes. This has been verified by numerical solutions of Eq. (4), assuming a constant oxidation reaction rate and neglecting the anoxic reactions and release of volatiles. However, if the heat flux at the surface were lower so that v is an order of magnitude smaller, the drying front would be roughly 10 cm from the surface of the coal and the time constant would be 6 to 7 hours. It appears then that the steady-state assumption is valid in the hotter regions of the coal block where coal is being consumed at a relatively rapid rate. However, other solutions may be required in regions where coal is not being consumed at the surface of the borehole.

## A SIMPLE EXAMPLE

The algebraic solution will be illustrated by the simple example of the burning of pure graphite, with dry air flowing in the borehole. The solution of this problem has already been outlined by Kays,[2] using a different derivation. Because the thermochemical properties of char are very similar to those of pure graphite, this is equivalent to setting $\rho_w$ and $\rho_{vol}$ to zero in Eqs. (12). With this simplification we get

$$h(T_2 - T_3) + gB_{O2}\Delta H_{or} = v\rho_6 C_6(T_3 - T_7). \quad (15)$$

The velocity v depends on the rate of consumption of carbon, $\dot{m}_c$, which is assumed to depend on mass transport of oxygen.

$$v = \dot{m}_c/\rho_6 = \eta g B_{O2}/\rho_6, \quad (16)$$

where $\eta$ is the mass of fuel consumed per unit mass of oxygen reacted. This can be substituted in Eq. (15) along with the relationship $h = C_2 g$, resulting in the cancellation of g and $\rho_6$. For convenience we will drop the subscript on B, change subscript 2 (referring to air) to a, and change subscripts 6 and 7 (both referring to unperturbed solid) to s.

$$T_3 = \frac{\Delta H_{or} + \eta C_s T_s + C_a T_a/B}{\eta C_s + C_a/B} \quad (17)$$

To estimate the temperature we still need to estimate B and $\Delta H_{or}$. The mass transfer potential, B, is defined by[2]

$$B = (P_\infty - P_0)/(P_0 - P_T), \quad (18)$$

where $P_\infty$ is the value of an appropriate conserved quantity in the airflow outside the boundary layer. Variables $P_0$ and $P_T$ are the same quantity an infinitesimal distance from the solid surface within the boundary layer and the solid, respectively. For the case of a simple surface reaction the appropriate expression for $P$ is[2]

$$P = m_C - \eta m_{O2}, \quad (19)$$

where $m_C$ and $m_{O2}$ are the mass fractions of graphite and oxygen. Because the vapor pressure of carbon is extremely low, $m_C$ will be zero in both the airstream and the boundary layer. If the reaction is limited by transport of oxygen across the boundary layer, $m_{O2}$ will be essentially zero at the surface and inside the solid. This gives $P_T = 1$, $P_0 = 0$, and $P_\infty = -\eta m_{O2}$, so that $B = \eta m_{O2}$.

The chemical products of the oxidation of carbon are CO and $CO_2$, in proportions which depend on the reaction conditions. If CO is the only product, the heat of reaction, $\Delta H_{or}$, will be 1690 calories per gram of $O_2$ reacted, the value of $\eta$ will be 3/4, and the value of B will be 0.174. If $C_s = 0.3$, $C_a = 0.25$ cal/g-K, and $T_a = T_s = 300$ K, then $T_3$ will be 1312 K. If $CO_2$ is the only product, then $\Delta H_{or} = 2970$ cal/g, $\eta = 3/8$, and $B = 0.087$, resulting in $T_3 = 1258$ K. The lower temperature with $CO_2$ as a product is somewhat surprising, because the heat of reaction per gram of $O_2$ is nearly twice as large. With the reaction rate limited by transport of oxygen across the boundary layer, the requirement for twice as much oxygen more than compensates for the larger heat of reaction.

Note also that the wall temperature does not depend on the heat transfer coefficients, because

they cancel. The physical picture of this is clear. If the mass transfer coefficient is larger the reaction rate will be increased, increasing velocity v, because carbon is being consumed faster. This increases the temperature gradient, and thus the heat transfer into the solid. Heat transfer into the gas is proportional to the mass transfer, so the temperature is independent of the value of the heat and mass transfer coefficients.

These calculated temperatures are just 100 to 200 K lower than the highest temperatures measured in the coal block experiments. In view of the differences between this calculation and the experimental conditions, this is surprisingly good agreement.

Equation (16) can now be used to calculate the velocity at which the coal surface moves. This requires that the mass transfer coefficient, g, be evaluated. Because $g = h/C_a$ we can use the extensive literature for evaluating h to obtain a value for g. In the coal block experiments the flow of air was 0.1 mole/s in a borehole with an initial diameter of 1 cm, yielding a Reynolds number around 4000. This is a little larger than the critical Reynolds number in a smooth tube, so we can use prescriptions for turbulent flow in tubes. The turbulent heat transfer coefficient is frequently expressed in terms of a dimensionless Nusselt number, Nu.

$$\dot{q} = h\Delta T = Nu(k/D)\Delta T ,$$

where k is the thermal conductivity of the medium (under static conditions) and D is the diameter of the tube, or the effective hydraulic diameter for tubes with noncircular cross section. Note that D/Nu can be interpreted as an effective thickness of the boundary layer, or sublayer. There is a great deal of experimental data, as well as approximate calculations, for evaluating Nu in the case of turbulent flow in pipes. When the flow is laminar Nu has its minimum value of 4.36. For turbulent flow, Kays[2] gives a semiempirical relation (his Eq. (9-26)),

$$Nu = 0.022Re^{0.8}\ Pr^{0.6}, \qquad (20)$$

where Re is the Reynolds number and Pr the dimensionless Prandtl number, which has a value of 0.7 for air. For Re = 4000, Eq. (20) gives Nu = 13.5, resulting in g = 0.0067. Using this value and $\rho_s = 2$ g/cm$^3$ for graphite gives $v = 0.44 \times 10^{-3}$ cm/s when CO is the only product. This is about half the average velocity observed in the coal block experiments. However, the density of the coals used in the experiment was about half that of graphite, and only about half of that is char; so we would expect higher velocities for coal. When $CO_2$ is the only reaction product, B will be half as large, so the velocity will be reduced. Considering that this example neglects drying and release of volatiles, the velocity is in good agreement with experiment.

Finally, we will examine the effects of radiation in this example. We will use Eq. (13), assuming a single surface at temperature $T_r$ with a view factor of 1.0. This gives

$$\dot{q} = \sigma(T_3^4 - T_r^4) .$$

Adding this term to Eq. (15) gives

$$T_3 = \frac{\Delta H_{or} + \eta C_s T_s + C_a T_a/B}{\eta C_s + C_a/B} - \frac{\sigma\left(T_3^4 - T_r^4\right)}{gB(\eta C_s + C_a/B)} \qquad (21)$$

The first term is the temperature with no radiation, as given in Eq. (17). The second term gives the effect of radiation. When $T_r$ equals $T_3$ the last term cancels. This is what we would expect if the surface is part of a hot cavity and can see only surfaces at temperature $T_3$. This will be a fair approximation for most portions of the surface of the borehole.

The effect of radiation will be most pronounced when $T_r$ is at ambient temperature, about 300 K. Using the values of the various parameters from above with $\sigma = 1.34 \times 10^{-12}$ cal s$^{-1}$ cm$^{-2}$ K$^{-4}$, we find that the radiation from the surface at 300 K adds about 6 K to $T_3$. The heat radiated from the surface of the coal reduces $T_3$ by around 400 to 500 K. Equation (21) can be solved by numerical iteration, and for the current example gives a temperature of 893 or 862 K when the product is CO or $CO_2$, respectively. These temperatures are too low for the chemical reaction to proceed at a sufficient rate to be self-sustaining, so the coal would not continue to burn. This is consistent with normal experience in burning wood, which burns much like

coal. A log will generally not burn unless some of the radiative loss is eliminated by nearby hot surfaces such as another log or a bed of coals.

## SUMMARY

The problem of modeling gasification in a coal block basically involves solution of a set of two-dimensional, time-dependent partial differential equations, which include species equations with chemical reaction terms. Certain approximations permit reducing the partial differential equations to ordinary differential equations: First, the gas flow is steady over times of several seconds, and the time constants for changes in the heat and mass transfer from the solid are at least this large, so the gas flow can be treated as steady-state and divided longitudinally into a number of control volumes. For each control volume of gas there is a corresponding washer-shaped solid zone and a boundary layer between the two. Heat and mass flow between the gas and solid are regulated by the boundary layer, as well as the properties of the gas and solid. In general, determining these flows requires solution of a time-dependent partial differential equation in the radial direction. This article has described a method of reducing the partial differential equation to algebraic equations using the assumption of a steady state due to movement of the hot surface of the coal resulting from chemical reaction. Estimates of the time constant show that the steady state assumption is reasonable at locations where the burning rate is high, but may not be so for colder zones. This requires further investigation. Although the partial differential equation can be reduced to algebraic equations, most of the complexity will come in handling the chemical reactions. This subject will be addressed in the immediate future. Radiative heat transfer must also be considered. Calculating the transfer coefficients should be straightforward, if tedious. The most likely complication arises out of the fact that the radiation will couple zones at some distance from each other, not just adjacent zones. This may introduce numerical instabilities which will have to be addressed. Including radiation is next in priority after the problems of the chemical reaction.

—J. Creighton

# PLAN FOR CAVITY BURN EXPERIMENTS IN LARGE COAL BLOCKS

One of the problems with UCG is that the early-time cavity development is not well understood. There is a different visualization for every mode. Burn experiments in small blocks of coal, conducted in 55-gallon drums, are beginning to provide information relevant to early-time cavity growth. A natural extension to larger blocks, perhaps 20 ft or more on a side, is now planned. The large block tests would be conducted at a mine, where blocks of coal would be isolated for use by the experimenter, or at LLNL using several blocks stacked or cemented together. The basic objective of the large block experiments is to quantify the early-time cavity growth at a scale large enough to allow safe extrapolation to field situations.

The Washington Irrigation & Development Co. (WIDCO) has offered to make large blocks available at its coal mine near Centralia, Washington. An agreement between WIDCO and DOE is in preparation. The preliminary cost estimate based on this plan totals $850,000. We expect the project to begin in April 1981 and end in October. Besides improving our general understanding of early-time cavity development in the UCG process, these experiments will provide us with information on which to base plans for a later large-scale UCG experiment in the same Tono Basin coal deposits.

The proposed tests should provide information concerning some of the following major technical questions.

- Does the burn cavity grow primarily because of coal drying and falling to the bottom, or is combustion on the solid walls most important? If coal collapse is important, at what cavity radius does it begin to dominate?
- Is there a relationship between the cavity aspect ratio (height to radius) and the gas flow rate?
- How does the linking channel behave as a function of flow rate? Is there a way of keeping it at the bottom of the seam, and does it matter?
- Do burns rise to the top in all coal seams?
- What flow rates, pressures, and injectant compositions should be used for gasification of WIDCO coal?
- What parameters control particulate production—only flow rate, or are there other factors?
- Is there an economical and reliable way to design the injection well so that the pipes survive? Does it matter?

The four tests we propose for the WIDCO site will not answer all of the questions listed above. That would take a long-term program involving many tests in several coal types. The specific goals for our plan are:

1. To determine the burn cavity shape and degree of rubble fill for a coal consumption of approximately 30 $m^3$.
2. To determine the gas composition and particulate production as a function of operating conditions through the burn.
3. To observe linking-channel growth due to hot gas flow.
4. To observe the extent of slag formation from parting zones and coal ash and determine any interactions with the burn process.
5. To determine any significant differences in cavity growth or process behavior due to changes in oxygen/steam ratio.

## DESCRIPTION OF THE EXPERIMENT

It is proposed that LLNL in cooperation with WIDCO perform gasification tests in drilled channels using oxygen-steam injection at an exposed coal face on the WIDCO property. Four experiments are planned, all similar in concept. A schematic cross section of the experimental arrangement is shown in Fig. 4. Figure 5 shows the experimental site in relation to the surrounding area.

A "drain-hole-type" drilling rig will be used to drill a horizontal hole parallel to the coal seam floor. A vertical hole will be drilled from above to intersect the end of the horizontal hole. The vertical hole will be cased and used as the production well. The initial part of the horizontal hole will be cased and used as the injection well. Ignition of the coal will take place at the end of the oxygen lance. Oxygen-steam will be supplied at slightly over atmospheric pressure to minimize gas leaks. Preburn pressure and flow tests will be used to find and seal any detectable leak paths at the coal face. An alternative configuration to the vertical production well

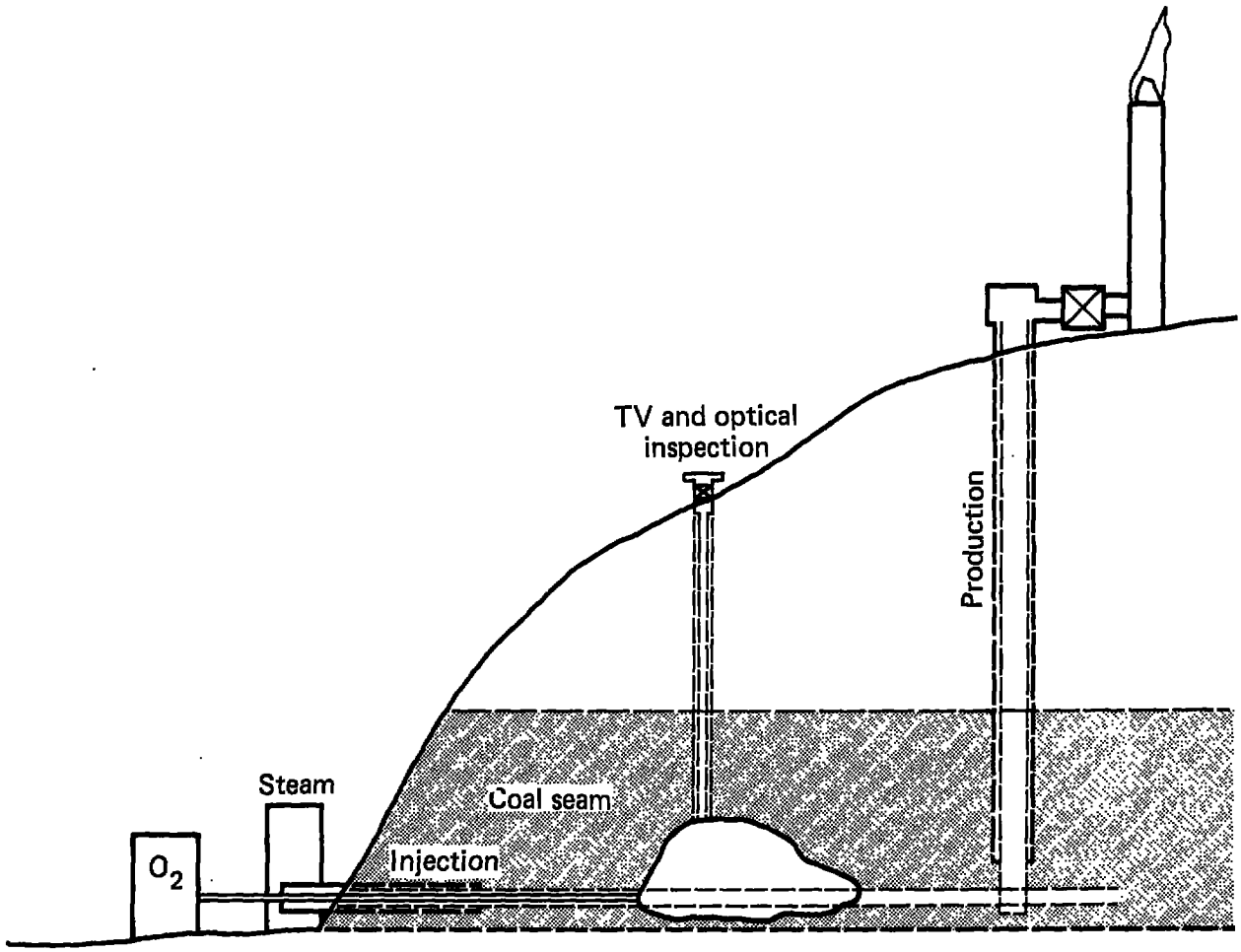


**FIG. 4. Schematic vertical cross section of the cavity burn experiments in large coal blocks proposed for the WIDCO site in the Tono Basin of Washington.**

is another horizontal hole drilled from the coal face, angled to intersect the injection channel. The choice of which option to use will depend on construction costs.

After ignition the coal will be gasified until approximately 30 $m^3$ of coal has been consumed. When the cavity has reached the desired size, the burn will be extinguished by turning off the flow of oxygen and steam and, if necessary, injecting water until the cavity has cooled to a safe level for inspection.

An inspection well, drilled before the burn, either vertically or from the coal face, will be used for visual cavity inspection. This well will be drilled to intersect the planned cavity and will be used with either a remote-controlled TV system or an optical periscope and range finder to observe and measure the cavity size. The inspection well will be equipped with a shutoff valve and an optical window for possible visual inspection and optical pyrometry during the later part of the burn.

After all four burns are completed, the burn cavities will be filled with cement grout and then excavated for further inspection and sampling.

Visual inspections and measurements of the burn cavities are expected to provide the most important diagnostic information from these experiments. The size and shape of the cavity, the condition of the walls, the degree and type of rubble or slag filling, and the state of the gas flow channel are all factors that can influence our ideas on the way the process operates.

Some real-time instrumentation will be used to diagnose the burn progress. A few thermocouple

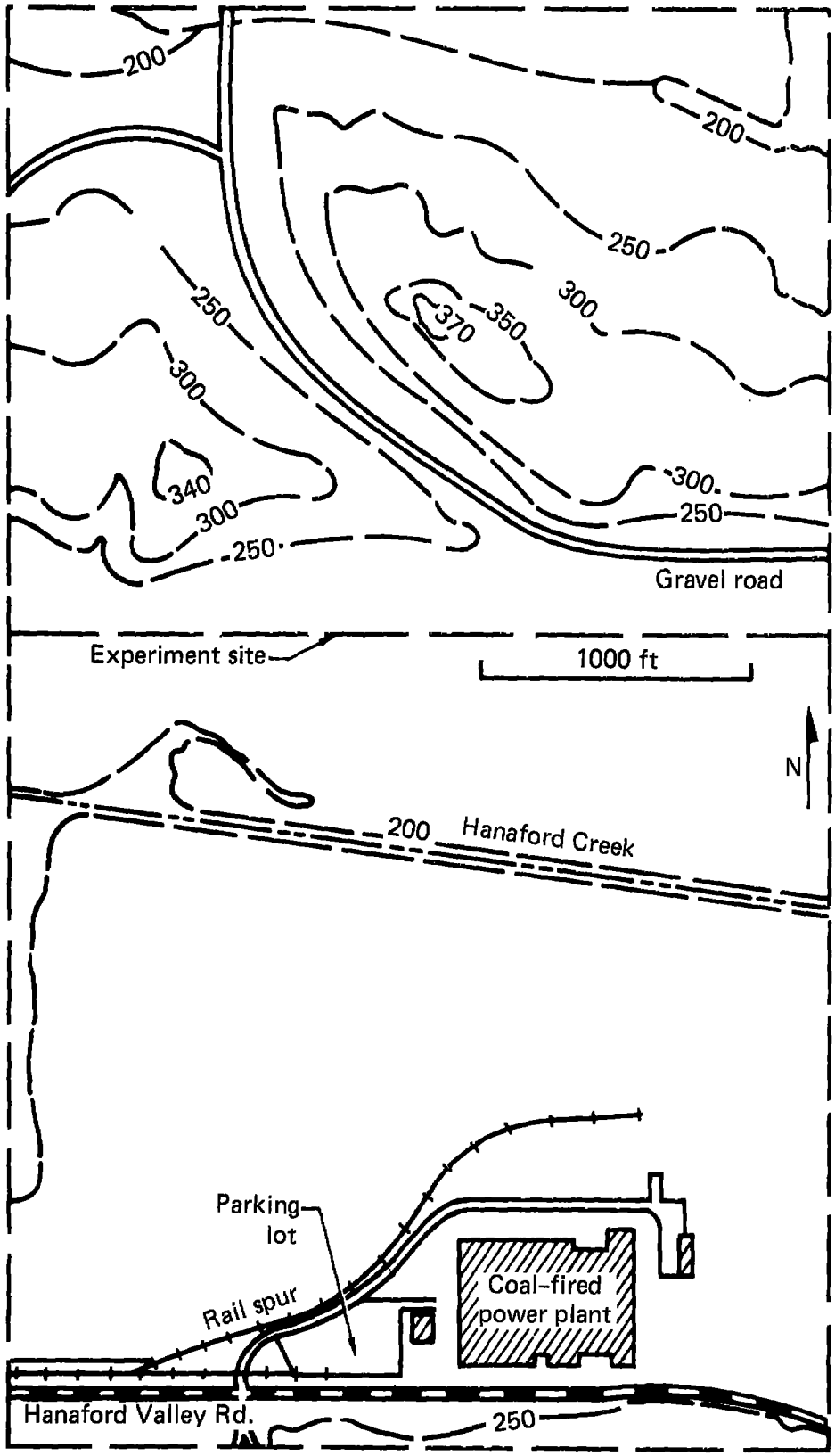


**FIG. 5. Area surrounding the site of the large block experiments.**

strings will be emplaced either horizontally or vertically (or both), depending on drilling costs. They will help us keep track of the gross features of the burn zone as a function of time. If funds are available, these four experiments would provide a good opportunity to calibrate the HFEM system and any other experimental thermal instrumentation under development. Standard measurements of gas chemistry, flow, and pressure will be made using the LLNL data acquisition facility.

Typical stratigraphy for the Big Dirty coal seam in the Tono Basin is shown in Fig. 6. Although the details will differ for the four experimental sites, the stratigraphy at the coal face is similar from one site to another in that many claystone parting layers of varying thickness are present. The burn cavity in each experiment will almost certainly intersect one or more clay stringers. This will provide data as to the importance of stringers in influencing cavity growth. The flow rates and steam/oxygen ratios will be varied in the experiments according to a predetermined schedule to determine their effect on cavity growth and gas composition.

## EXPERIMENTAL STRATEGY

Four experiments are planned: three in the main part of the coal seam with as uniform a stratigraphy as possible, and one near the top of the coal seam so that the cavity will reach the roof and begin to interact with it. The first three experiments will test the effects of flow rate and steam/oxygen ratio on cavity growth. We will vary the injection flow rate so that it is proportional to the square of the operating time. This will maintain a constant oxygen flux per unit area of cavity, and also a constant gas velocity.

The choice of a squared time dependence for flow rate is somewhat arbitrary but was developed from the following arguments. First, it is clear that, within certain limits, flow rate should increase as the reaction volume increases. Certainly this is obvious if one considers the extreme cases of very low flows for an enormous volume and, conversely, extremely high flows for a very small volume. Secondly, we recognize that this test is midway in scale between the very small laboratory tests and the large-scale field tests, and hence it may serve a useful function in tying all the tests together. We hope ultimately to be able to do this tying-together with our modeling effort, but currently we do not feel an adequate model is available. Consequently we have considered a simplified approach where one parameter is singled out as a candidate for scaling purposes.

We have considered parameters such as Reynolds number, Froude number, constant velocity, constant oxygen flux, constant residence time, and others. We can further assume that some single value of the chosen parameter is optimum over the course of the experiment. This leads, after a number of other simplifying assumptions, to the conclusion that the flow rate should, in general, be scheduled according to $f = kt^n$, where f is the flow rate, k is a constant, t is time, and n varies according to the parameter chosen. (The exception to this type of time dependence, for the parameters considered, occurs with the assumption of constant residence time, which leads to an exponential time dependence.)

This simple flow relation is attractive for several reasons. First, it generally allows one to prescribe a nonarbitrary flow-rate schedule for a single experiment; it focuses on changing a single parameter, k, from experiment to experiment; and finally, it gives a method of scaling experiments. Our choice of $n = 2$ was a result of our feeling that, of the simple parameters explored, the constant oxygen flux seemed to have the most merit, and the resulting scaling between small and large experiments seems to fit naturally within the framework of the operating experience we have had. Of course, as we gain more experimental and modeling evidence we may modify the simple $f = kt^2$ schedule.

Each experiment will be continued until 27 $m^3$ (40 tons) of coal has been consumed. The resultant cavities should be large enough to illustrate most of the conditions to be encountered in the first few days of an underground test. The first two experiments will be done with the same oxygen/steam ratio but with different maximum flow rates. The third experiment will duplicate one of the previous flow-rate schedules but with a different oxygen/steam ratio. The fourth, or roof-interaction experiment, will use the same oxygen/steam ratio and flow rate shedule as one of the first three tests. The pertinent flow rates and operating times are given in Table 3.

High particulate emission or oxygen breakthrough at the production well may make it

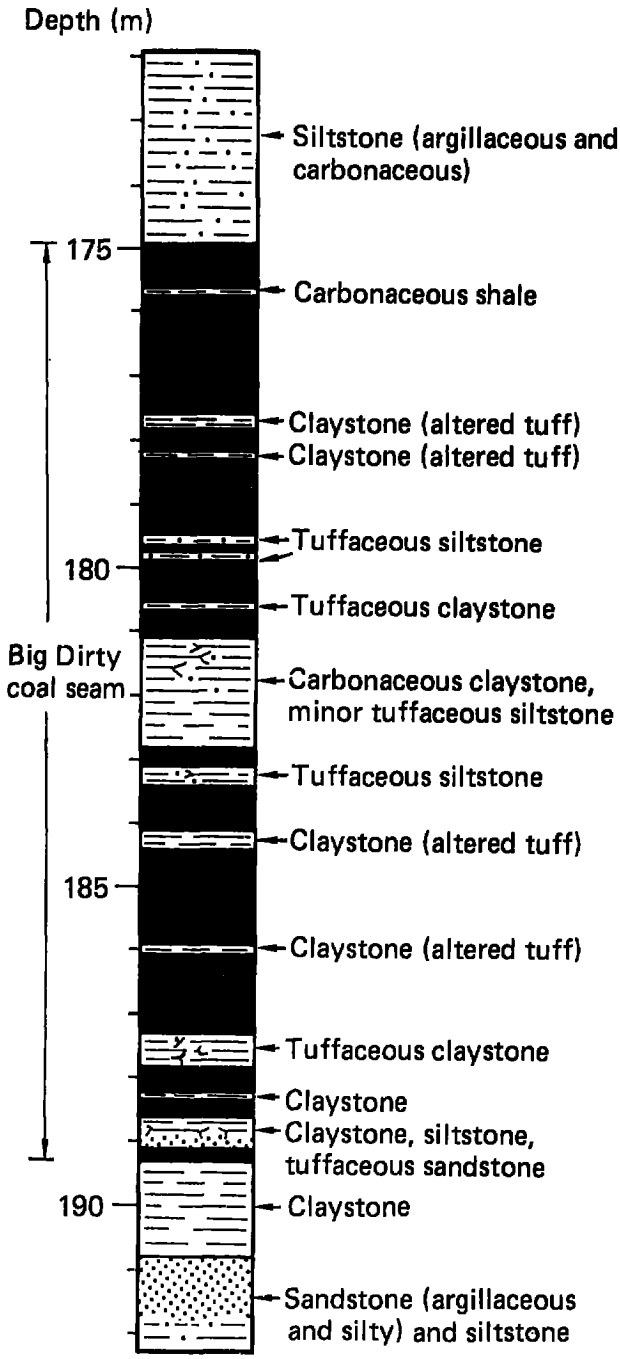


**FIG. 6. Stratigraphy of the Big Dirty coal seam in the Tono Basin, at borehole DOE-5.**

**TABLE 3. Planned burn times, flow rates, and steam/oxygen ratios.**

| | |
|---|---|
| Time for fast flow experiment | 2.9 days |
| Maximum oxygen flow rate | 5.05 mol/s |
| Time for slow flow experiment | 5.8 days |
| Maximum oxygen flow rate | 2.53 mol/s |
| Coal consumed in each experiment | 27 $m^3$ (40 tons) |
| Steam/oxygen ratios | 2/1 and 4/1 |

necessary to change the planned flow-rate schedule. The purpose of these tests is to learn about burn cavity formation, so the results of one test may very well modify our plans for the next test.

## COMPONENT SYSTEMS

The processing systems designed to support the series of experiments will consist of conventional components mounted on portable or temporary structures for easy installation and assembly. These components will provide for supplying injection gases to the process, controlling critical parameters, and disposing of exhaust gases generated within the gasification reaction zone. Auxiliary systems will include a conditioning (cleanup) system for the produced gas, to accommodate an on-site gas analysis installation, and a cooling/quenching water system to control high-temperature zones that may pose the threat of thermal damage to components.

### Injection Gas Systems

The two injection gases—steam and oxygen—will be supplied to the experiment from trailer-mounted and/or mobile units. Steam will be provided by a trailer-mounted steam generator rated at approximately 50 boiler horsepower. This unit will produce 1500 lb/hr of steam at pressures adequate to supply the process (50 psia). A portion of this steam flow will be available for vaporizing liquid oxygen for process purposes. The oxygen will be delivered to the site in liquid form by transport trailers. A trailer-mounted vaporizer will be used to supply the required flow of gaseous oxygen to the system. This unit will be heated either by steam or electricity.

Both steam and oxygen will be supplied to the process through flow-control systems using standard control valves and orifice flow metering. Remote and automatic control of the system will be available from a control facility located at a convenient distance from the coal seam face.

### Process Wells

The injection wells will consist of horizontal channels drilled into the coal face. These boreholes will be cased over a distance of at least 20 ft. Wellheads will be assembled to the surface ends of the well casings. Each drilled channel, beyond the end of the casing, will serve as the main path for development of the gasification channel and growth of the cavity. These channels will communicate directly with the bottoms of the production (exhaust) wells, as shown in Fig. 7.

The production wells will be drilled and cased from the surface to well within the coal seam. Each well will be drilled beyond the end of the casing to the base of the coal seam to intersect with the horizontally drilled injection channel. Exhaust gas piping will be connected to the wellhead attached to each production-well casing string.

### Exhaust Gas System

The produced gas flowing from the production wells will be manifolded together into a common stream to accommodate backpressure control and flow metering. Redundant, parallel flow-metering stations are used to provide for wide fluctuations in flow and to accommodate on-line replacement of orifice plates, etc.

The produced gas will be disposed of in an incinerator, in which the gas and combustion air are introduced through nozzles in the base of a 30-ft, refractory-lined combustion stack. This unit is designed to burn approximately 3000 cfm of gas of the quality expected to be generated from the experiments (120–180 Btu/scf).

### Water System

A source of water will be available at the site to provide for the various requirements. The process wells will be equipped with ports through which cooling water will be introduced if the well temperatures indicate the need for control; this system will also be used to quench the gasification process at the time gasification is to be terminated. In addition, the water source will supply boiler feedwater for the steam generator.

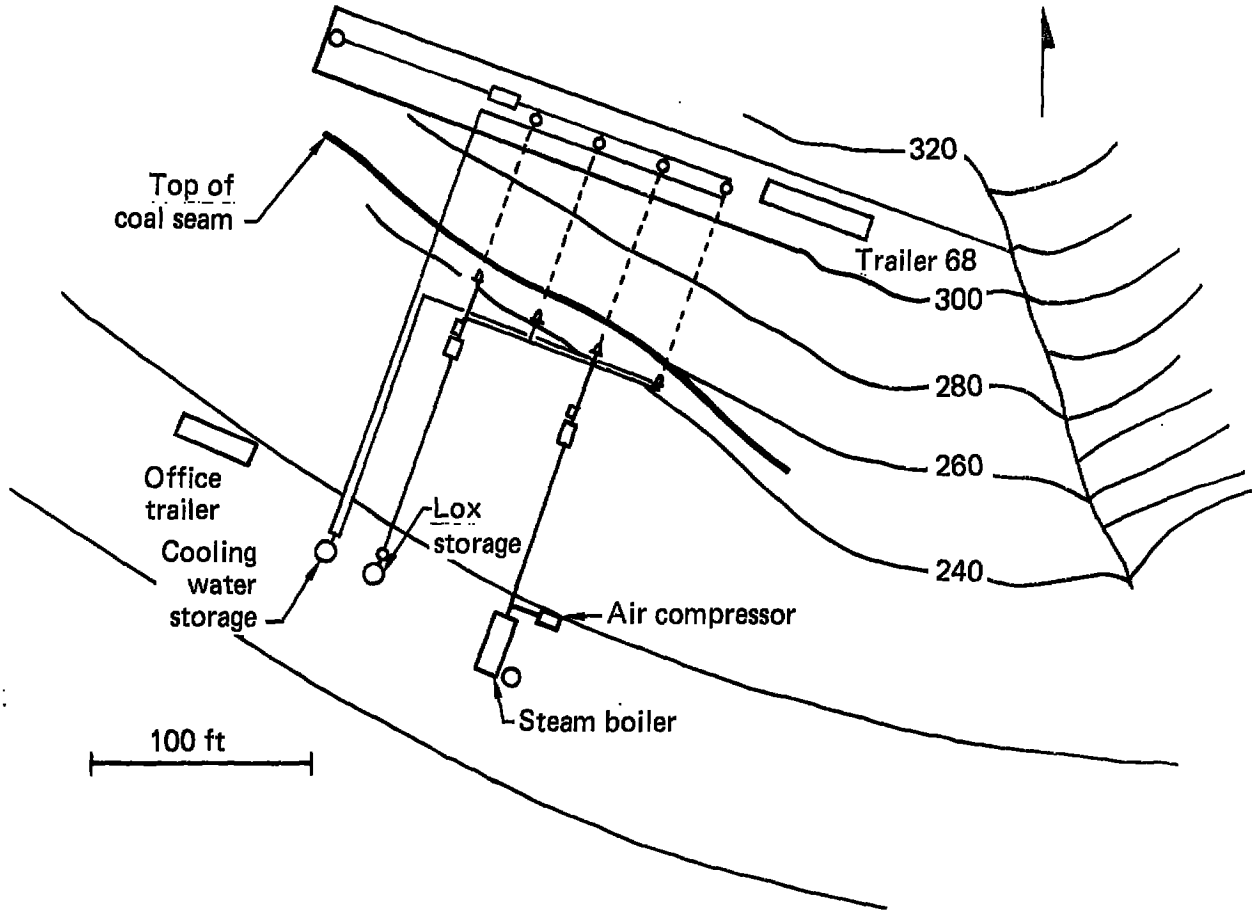


**FIG. 7. Plan view of the experimental layout for the large block experiments.**

### Temperature Monitoring System

The most significant diagnostic variables to be monitored during the tests will be the temperatures in the various gas streams and within the burn zone. These temperatures will be monitored with thermocouples, most of which will be embedded in the coal seam through separately drilled channels or attached to the casing or other internal parts of the process wells. The temperature measurements will be displayed and recorded in the control facility and will be used to continuously observe growth of the gasification reaction zone cavity.

### Schedule

A tentative schedule is shown in Fig. 8, with a starting date of June 22, 1981, assuming all permits and contracts are obtained.

## FUTURE TESTS

The availability of this exposed coal face for testing purposes makes possible a whole new series of relatively inexpensive tests. Progress in underground gasification design could be speeded up by several years if this option is pursued vigorously.

Some tests would require only a few days, while others might last for two or three weeks. Perhaps 10 to 20 such tests could be completed for the cost of one major *in situ* test such as the proposed Tono 1.

—R. W. Hill
C. B. Thorsness
D. S. Thompson
R. J. Cena
M. J. Shannon
D. R. Stephens

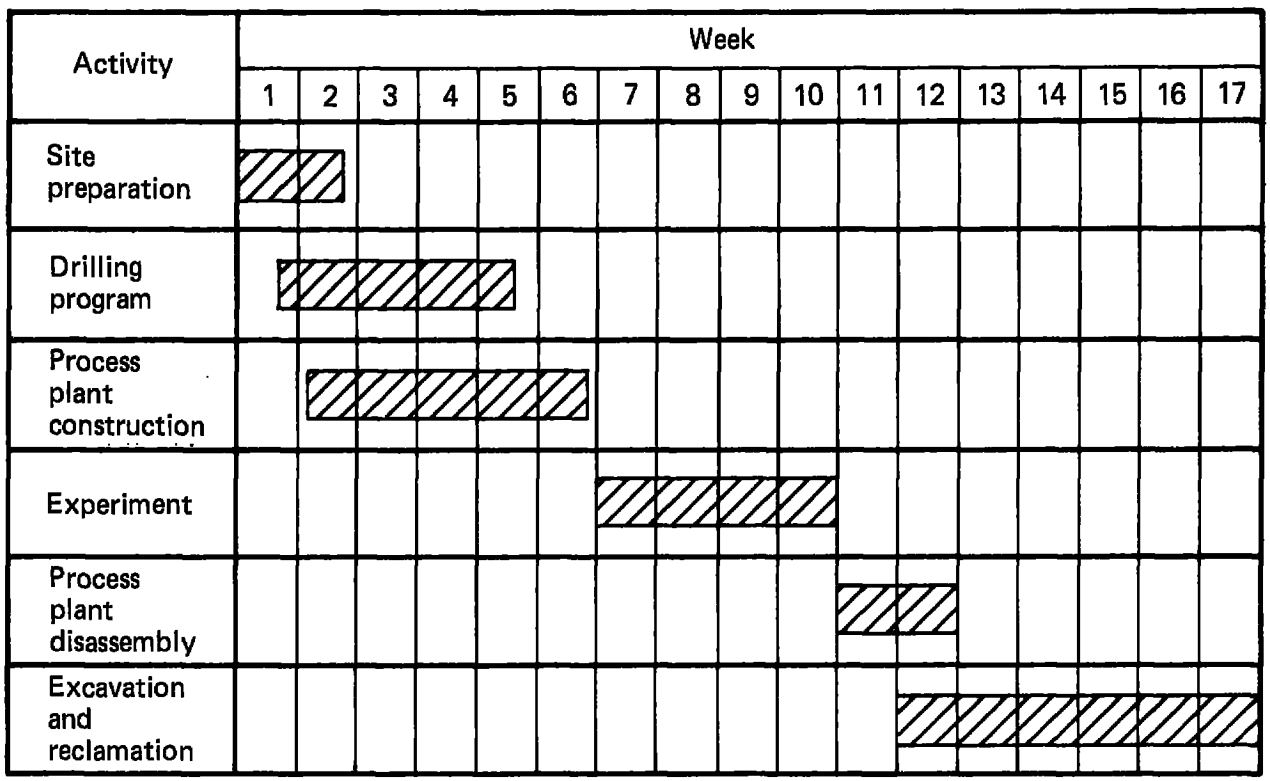


**FIG. 8. Tentative schedule for the large block experiments.**

# POSTBURN CONDITION OF UCG PROCESS WELLS

## CORING THE COLLAPSED ZONE OF WELL P-1 AT HOE CREEK NO. 3

As a final activity connected with the postburn coring of the Hoe Creek No. 3 burn zone, we investigated the lower collapsed zone of process well P-1. We used the standard wireline coring system, and began coring at 142 ft below the surface. It was at this depth, near the bottom of the Felix No. 1 coal seam, that the well casing had failed. With the exception of a narrow layer of soft clay at the 160-ft depth, the core displayed a high degree of thermal alteration. Slag from roof material intermixed with metallic oxides and small pieces of metal, mostly copper, was found throughout the cored zone down to a depth of 171 ft, where unaltered Felix No. 2 coal was encountered. (The core borehole had drifted outside the originally drilled path of the well.)

Of significance in these observations is that no remnants of the original casing or casing liner were found. This suggests that rather severe corrosive conditions, accelerated by high temperatures, were imposed on the injection well. We assume that the metal members failed as a result of oxide corrosion which took place at a high rate of attack, driven by the higher temperatures resulting from the oxygen-steam processing.

## LOGGING THE HANNA II PROCESS WELLS

The LLNL logging truck, which was in the area to support the postburn coring work at Hoe Creek No. 3, was used to take a cursory look at the postburn condition of the Hanna II process wells. On August 15, 1980, natural gamma and caliper logs were run in all four Hanna II process wells. The interpretation of stratigraphy from the gamma logs, when compared with a known undisturbed stratigraphy, was inconclusive for purposes of detecting overburden movement. However, the caliper logs did yield a mild surprise in that the wells were found to be in such good structural condition. Figure 9 shows graphically how these wells survived the gasification process. Of particular note are the following observations:

- All the wells remained intact for a considerable distance into the coal seam.
- Well No. 6, used as an injection well (in phase 2), shows nominal gauge diameter through the entire seam.
- Two of the wells, Nos. 5 and 6, show what might be casing separations at collars within the coal seam, at depths of 272.5 and 289 ft respectively.

—D. S. Thompson

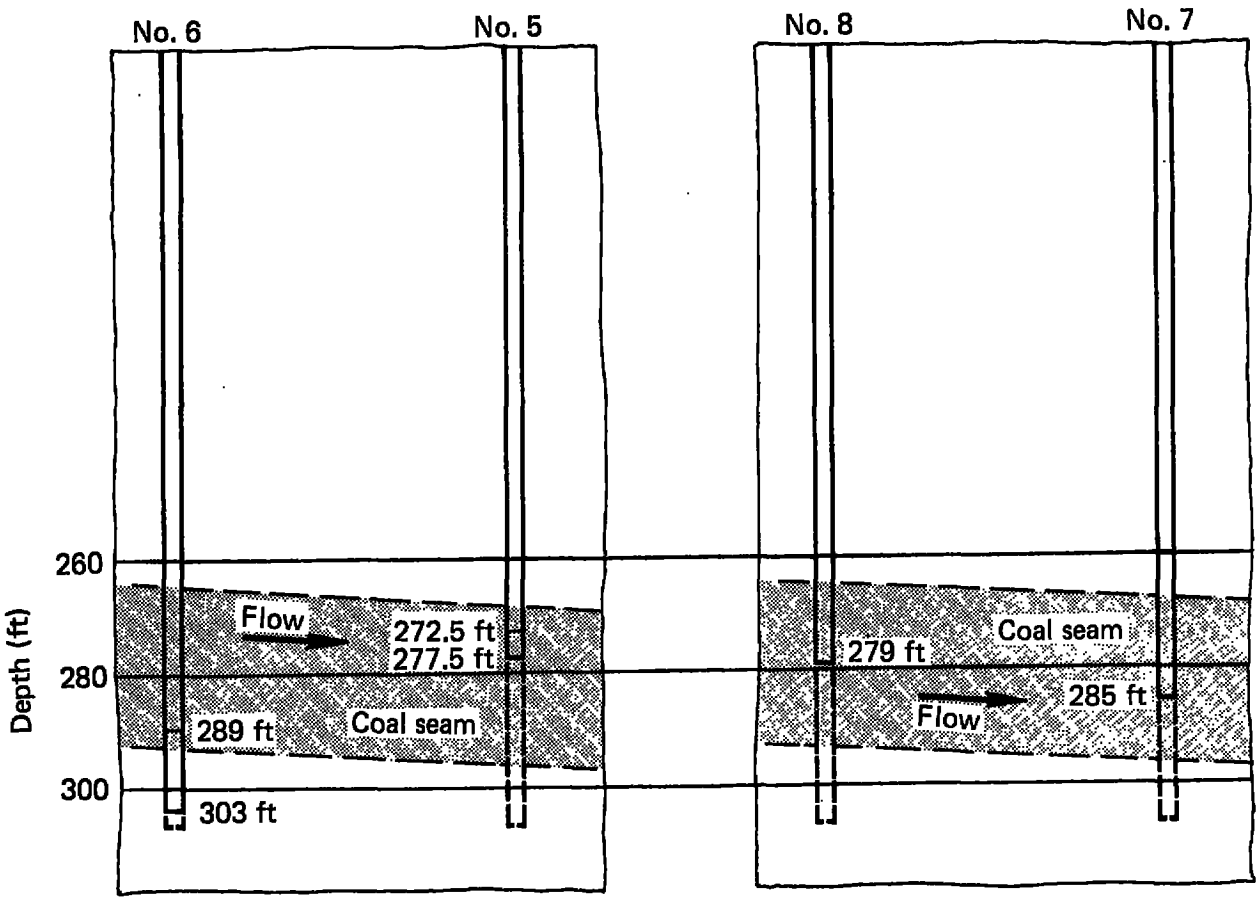


**FIG. 9. Condition of the Hanna II process wells after the gasification experiment. Portions of the wells that remained intact after the experiment are shown by solid lines. Portions of the wells that did not survive the experiment are shown by dashed lines.**

# PLAN FOR DIRECTIONALLY DRILLED BOREHOLE FOR THE DOE EXPERIMENT NO. 1 WITH WIDCO IN WASHINGTON

Conventional tooling will be used for construction and completion of the directionally drilled injection well for DOE Experiment No. 1. This will impose normal oil-field industrial limits on hole size, maximum deviation rate, directional control, and casing point locations.

The azimuth of the injection well link as shown in Fig. 10 corresponds to a convenient preliminary layout of the two production wells, 1B and 1C. If follow-on site characterization data show fault lines or high permeability zones in locations inconvenient for this layout, appropriate changes to the azimuth line will be made.

Figure 11 is a sketch in vertical cross section of the path to be taken by the directionally drilled hole. In general, the purpose served by the construction of this hole will be to provide (1) a low-point path for injection gases introduced into the coal seam and (2) a drilled link between injection and exhaust points within the coal seam. This link is necessary to support combustion and gasification of the coal in the reaction zone.

## DRILLING EQUIPMENT

The drill rig employed for this work will be a top-head-drive unit with slant-drilling capability. Tooling will include conventional drill rod and tricone bits as well as flush-coupled casing and downhole mud motors to accommodate directional

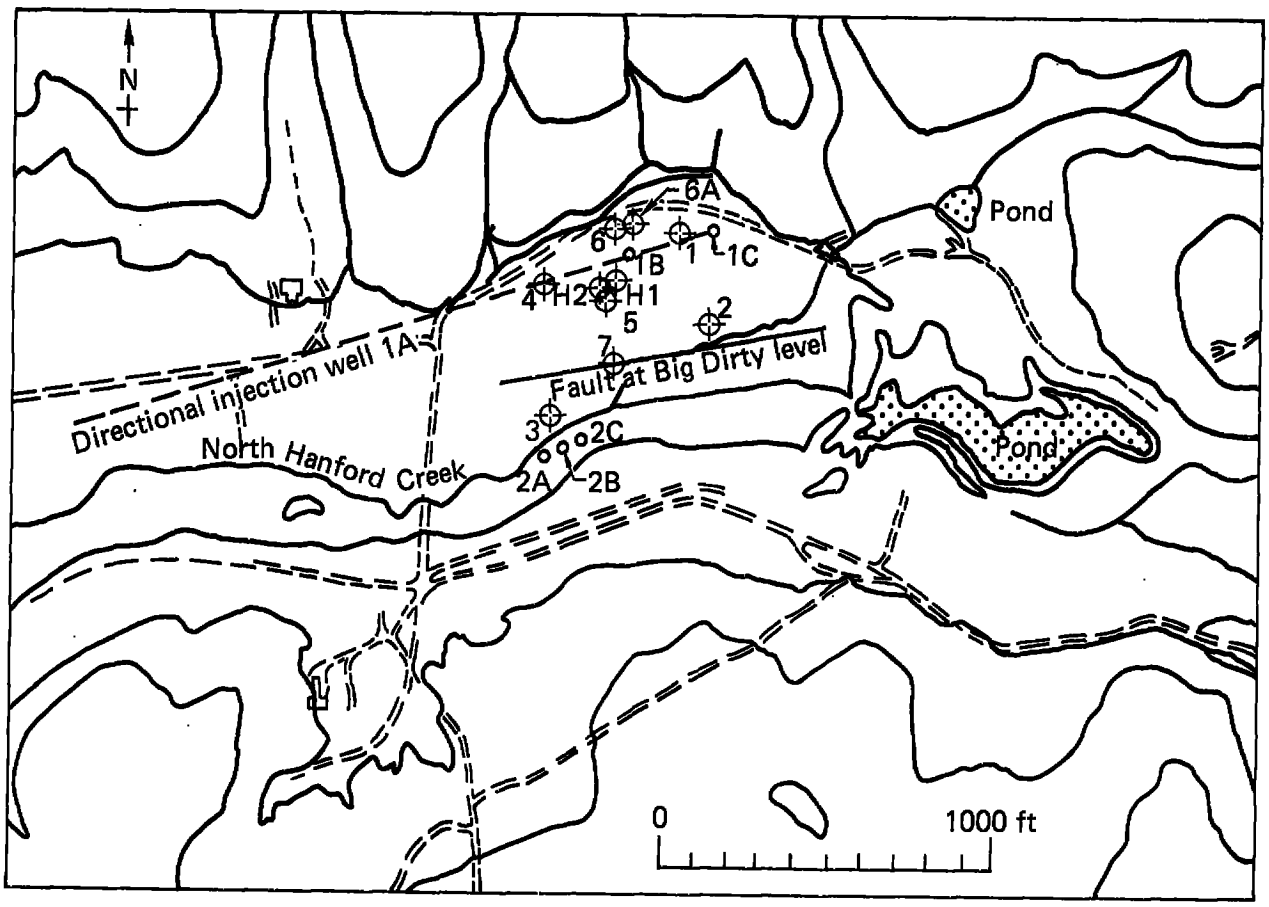


**FIG. 10. Site map for DOE Experiment No. 1 in the Tono Basin of Washington, showing tentative location of the directionally drilled injection well.**

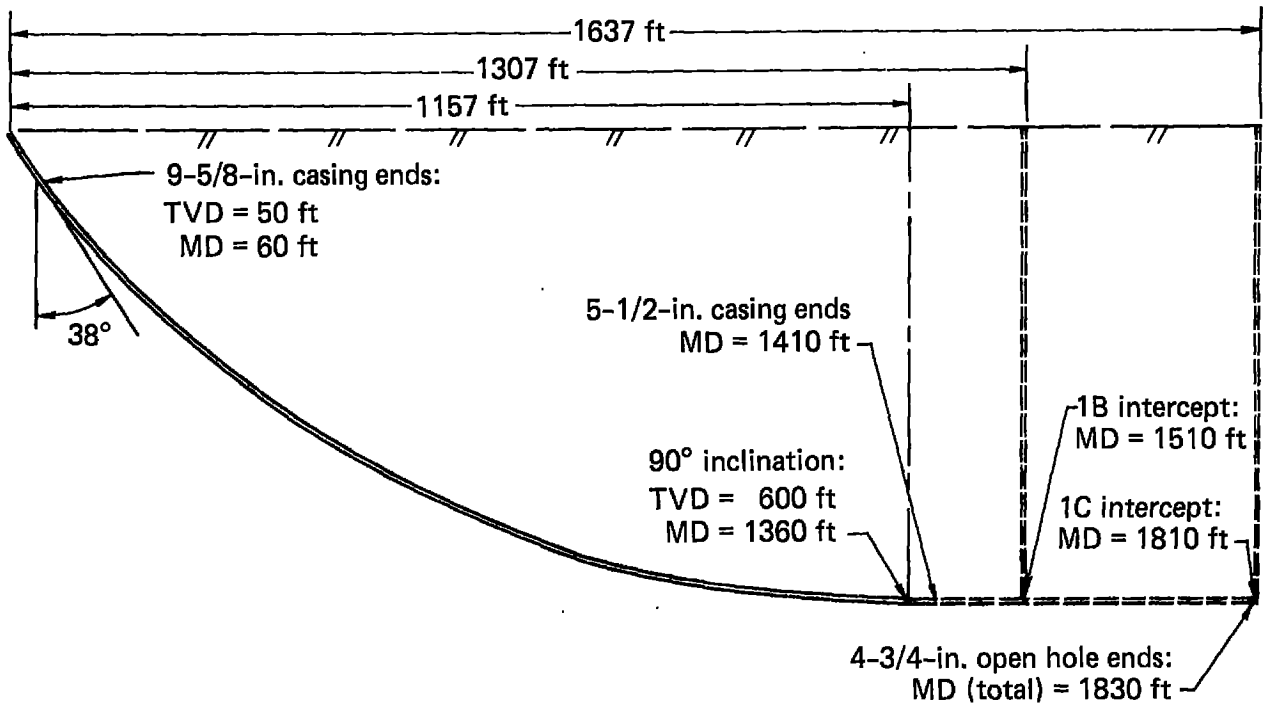


**FIG. 11. Schematic vertical cross section showing the proposed path of the directionally drilled injection well for DOE Experiment No. 1 in the Tono Basin. TVD = total vertical depth of hole, MD = measured depth (i.e., length) of hole.**

control. Downhole directional surveying tools will include magnetic single-shot (wireline) and gyro-stabilized units. A completely enclosed mud-recirculating system will be used to assure drilling fluid control for purposes of stabilizing and cleaning the hole as drilling progresses.

The drilling operation will involve a three-man crew plus one supervisor on each shift, and will continue on a 24-hour-per-day basis.

## DRILLING PROGRAM

Entry angle for the rig (at the surface) will be approximately 38° from vertical. Spud location will be approximately 1300 ft upstream from the point of intersection with the first vertical production well (1B). Azimuth will be approximately N70°E. All these data are preliminary and tentative, and will be firmed up after completion of the characterization program.

### Setting Surface Conductor

Approximately 60 ft of 9-5/8-in. surface conductor will be emplaced. A pilot hole will be drilled using standard rotary techniques and tooling. The pilot hole will be reamed to approximately 12-in. diameter. The casing will be run with centralizers and cement shoe and then cemented to the surface.

### Drilling Deviated Pilot Hole

Using a combination of conventional rotary and downhole-mud-motor drilling systems, a small pilot hole (approx 3-1/2 to 5 in. in diameter) will be drilled. Starting at the base of the surface conductor, the hole inclination will be gradually increased from 38° to 90° at a building rate of approximately 4°/100 ft. The slanted section of the hole before the inclination reaches 90° will involve drilling approximately 1300 ft along the path of the hole and a drop in elevation of approximately 550 ft. Mud motor orientation and bit pressure will be used to control angle building rate and azimuth. Directional surveys will be made every 10–20 ft along the drilled path as drilling progresses.

Upon reaching the 90° drift point, near the bottom of the coal seam, the directional hole will be straightened and held along a horizontal path for approximately 50–100 ft.

### Running Injection Well Casing

The approximately 1350 ft of directional pilot hole will be reamed to about 8-in. diameter over its entire length. Casing will be run in with centralizers

and cement shoe. Tentative size of the casing is 5-1/2-in. diameter. Cement will be run to the surface with a special high-temperature mix spotted along the lower 150 ft of the casing. Cement pumping through the casing will be done using pressures low enough to preclude hydraulic fracturing of the coal and overburden formations.

**Extending Horizontal Link**

Horizontal drilling along the base of the coal seam will be attempted with conventional rotary equipment and techniques. Special stabilizers will be required to keep the path of the hole following the bottom contour of the coal seam. If directional control with rotary tooling is not adequate, the mud motor system will be reemployed. This linking hole, regardless of the drilling system used, will run horizontally for a minimum distance of 420 ft. The gauge of the hole will be approximately 4-3/4 in.

Completion of this section of the hole will complete the drilling program for the injection well. Drilling of the remaining process and diagnostics wells will be done as part of a later and separate drilling program.

**Schedule**

It is anticipated that the drilling program briefly outlined above will be accomplished in roughly two months of on-site operations. This includes all necessary mobilization and demobilization effort, running of casing, and cementing operations.

—D. S. Thompson

# ANALYSIS OF BURN CAVITY GROWTH IN HOE CREEK NO. 3

One of the goals of the U.S. Energy Program is to develop new methods for producing clean fuel from coal. Underground coal gasification is one of the more promising of these processes. Its technical feasibility has been demonstrated repeatedly by field tests in this country and abroad. The challenge now is to develop a reliable, repeatable process that can be economically competitive with other methods of utilizing our coal resources.

Here we summarize some of the results from the third LLNL *in situ* coal gasification experiment at Hoe Creek, Wyoming.[3] The experiment employed a directionally drilled channel between process wells spaced 130 ft apart. Over 4200 tons of coal was consumed in a 57-day gasification period. During the 47 days of oxygen-steam injection the average heating value of the gas produced was 217 Btu/scf.

The *in situ* process is, by its very nature, extremely difficult to observe. The mechanisms involved in burn cavity growth are not well understood because of this observational difficulty. The Hoe Creek No. 3 experiment was heavily instrumented to provide cavity growth information. There were 15 thermocouple wells, each containing an average of 14 thermocouple junctions spaced at intervals throughout the coal seams and overburden. Additional thermocouples were fastened to the outside of all the process well casings. The thermocouple wells were designed to monitor the progress of the burn down the channel and also to define the boundaries of the burn cavity during the last two-thirds of the experiment.

Eight wells were used to monitor burn cavity growth during the early stages of the experiment by the HFEM (high frequency electromagnetic) technique. This technique utilizes changes in transmission of an rf signal caused by heating and burning of the coal. Radio transmitters and receivers are placed in the wells, and the signals are recorded on the surface.

Five extensometer arrays were installed to measure the motion of the overburden layers at various points.

Fifteen core holes were drilled after the experiment to define the final cavity configuration.

The results from these four different diagnostic systems have been combined to produce a description of the shape of the burn cavity as a function of time. Some of the highlights of this analysis are as follows:

1. Although the Felix coal at Hoe Creek is split into two seams by a 15-ft-thick parting zone, both seams were consumed.
2. The injection wells were installed with the bottom of the casing close to the bottom of the lower seam. Gradual burning off of the casing eventually moved the injection point to the top of the upper seam for both of the injection wells used. This resulted in more coal being consumed from the upper seam than from the lower.
3. Slag buildup in the bottom of the burn cavity apparently prevented any downward progress of the burn zone below the original channel level.
4. Good correlation is seen between roof collapse events and product gas quality and temperature.

The cavity development is illustrated by the following figures.

Figure 12 illustrates the three basic signal types from an HFEM scan: No. 1, no cavity; No. 2, small, hot burn cavity; and No. 3, large, cool cavity where transmission through the void is greater than the attenuation.

Figure 13 is a simple map showing the locations of the process wells and some of the instrument holes at Hoe Creek No. 3. The thermocouple wells I-5, I-12, and I-15 played a major role in the analysis. The vertical planes scanned by HFEM surveys are indicated by the dashed lines joining pairs of wells at the left side of the figure.

Figure 14 is a more detailed map of the experimental site, including all of the instrument holes used for the experiment, as well as the postburn core holes from which the final shape of the cavity was determined.

Figures 15–21 show the burn cavity in plan and elevation views for different days throughout the burn. Forward gasification started on day 229 and ended on day 283. The injection well used and the injectant (whether air or oxygen-steam) are indicated on each figure, along with the day.

The contours were derived from a consideration of all the data available: HFEM, thermocouple, extensometer, and mass balance, as well as the

(Continued on p. 35)

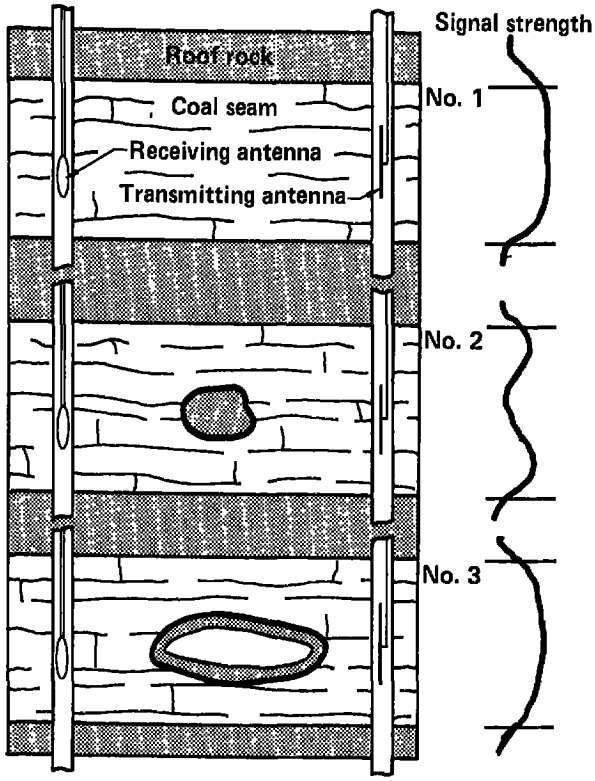


**FIG. 12. HFEM scans between holes can indicate anomalies such as cavities in the intervening material. Three typical transmitted HFEM signals are shown here: No. 1, no cavity in the intervening material; No. 2, a small hot cavity; No. 3 a large cool cavity.**

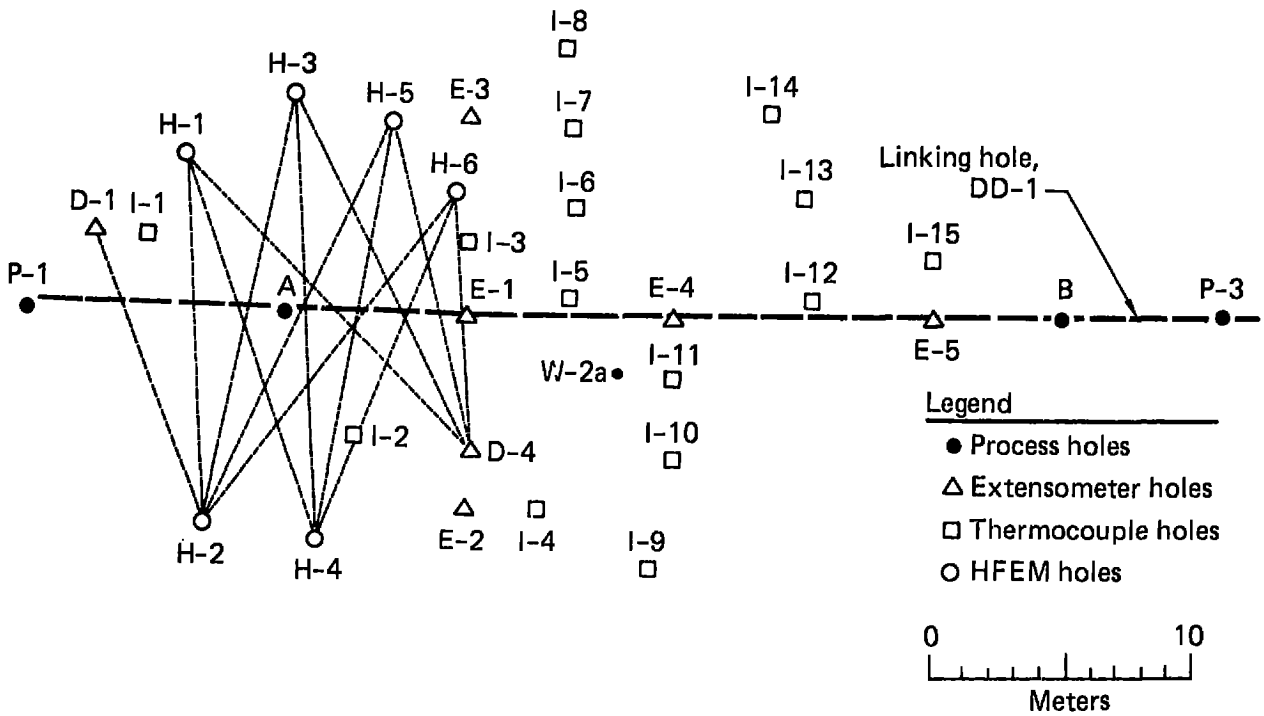


**FIG. 13. Plan view of some of the instrument and process wells for Hoe Creek No. 3. Dashed lines between well pairs show where the HFEM scans were made.**

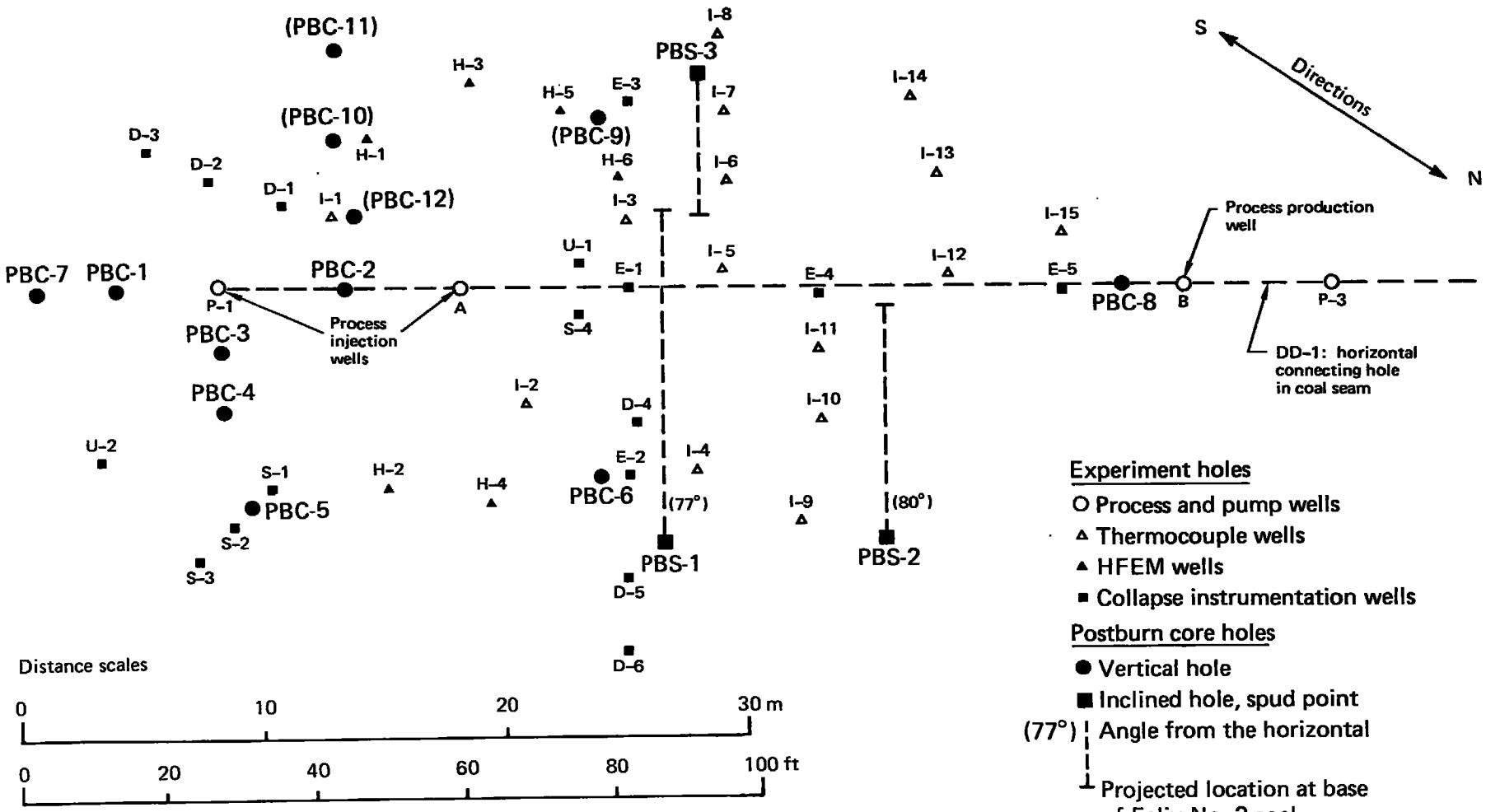


FIG. 14. Detailed plan view of Hoe Creek No. 3 site, including postburn core holes.

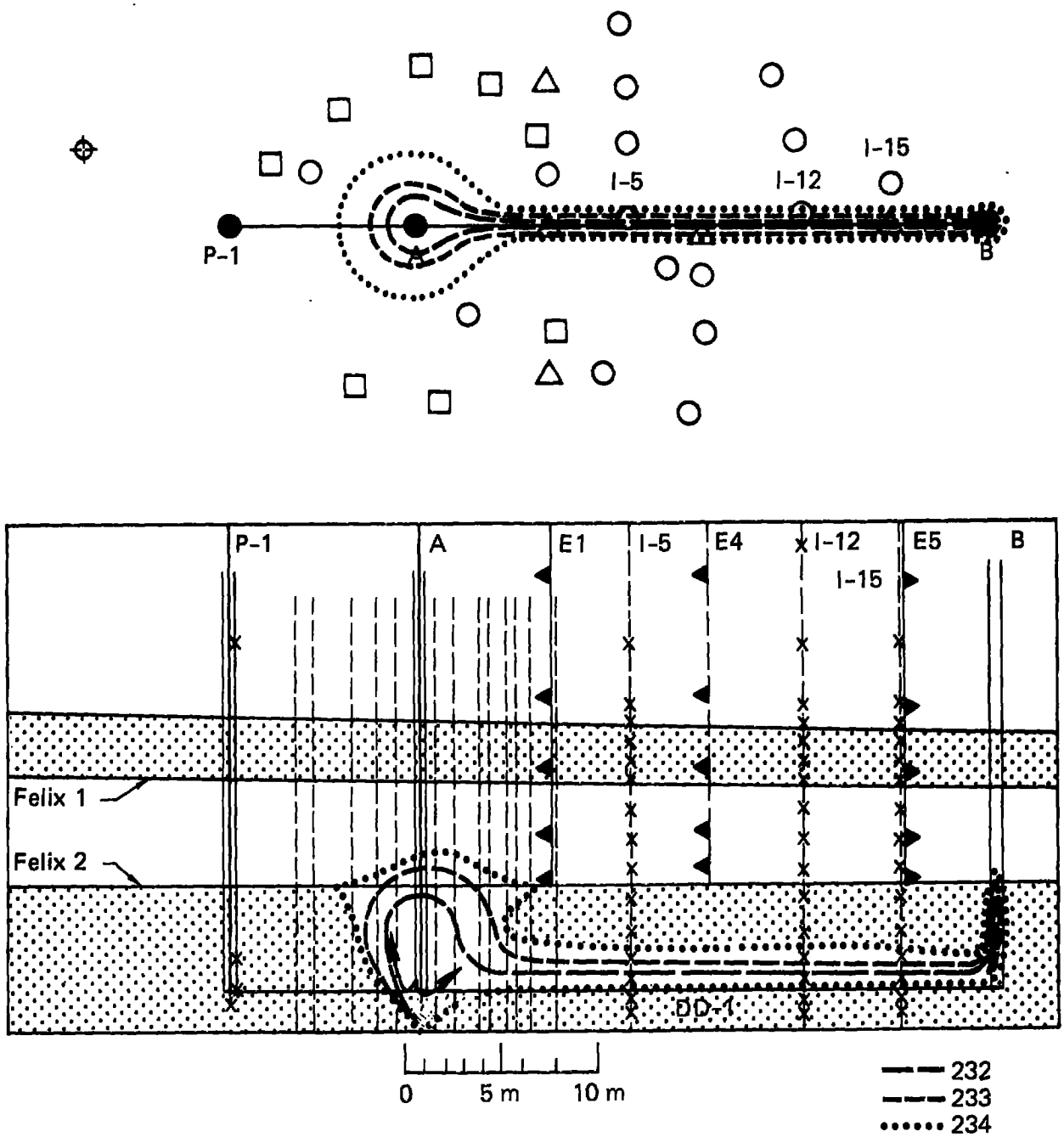


FIG. 15. Hoe Creek No. 3 burn cavity at days 232, 233, and 234.

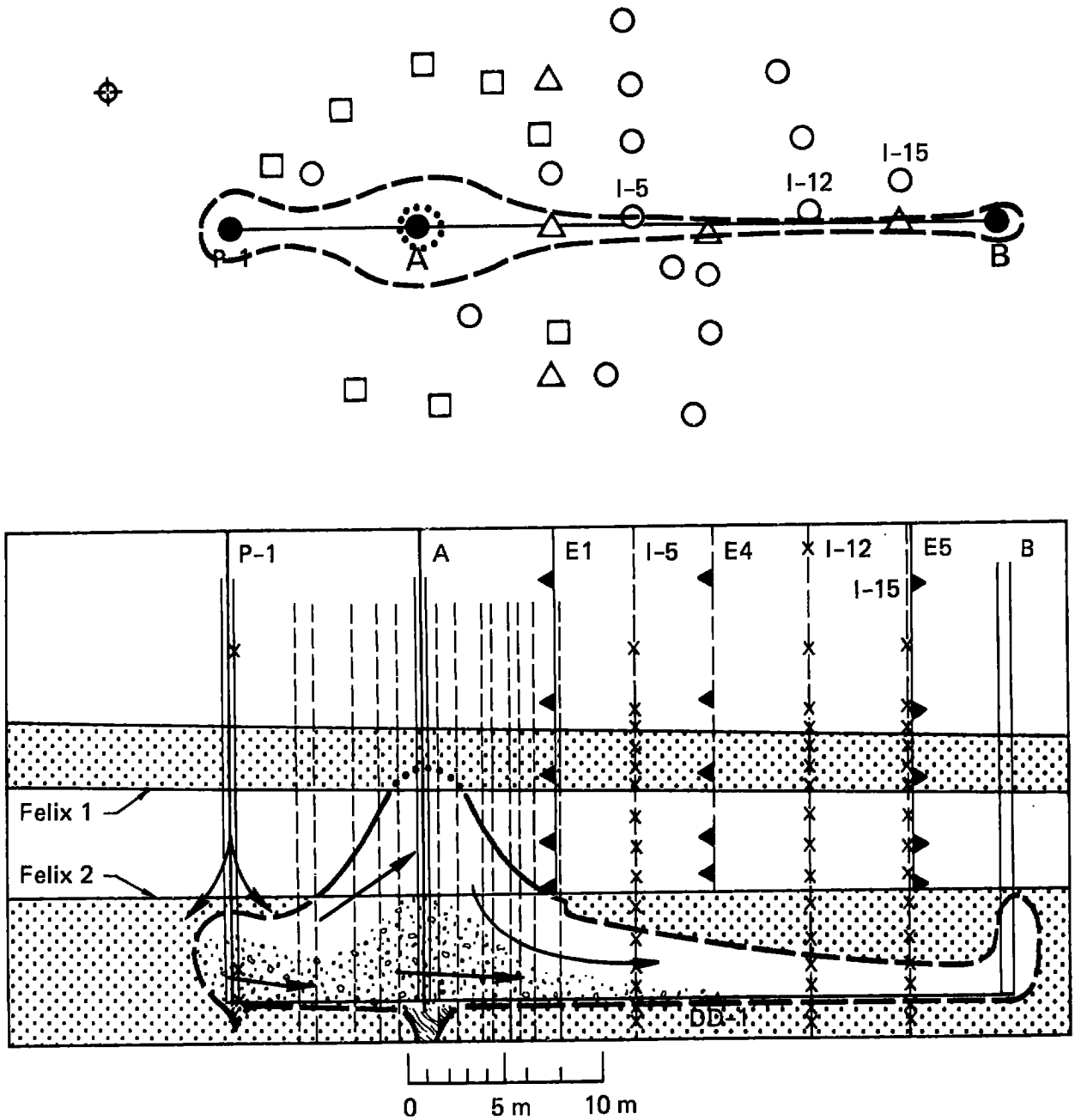


FIG. 16. Hoe Creek No. 3 burn cavity at day 238.

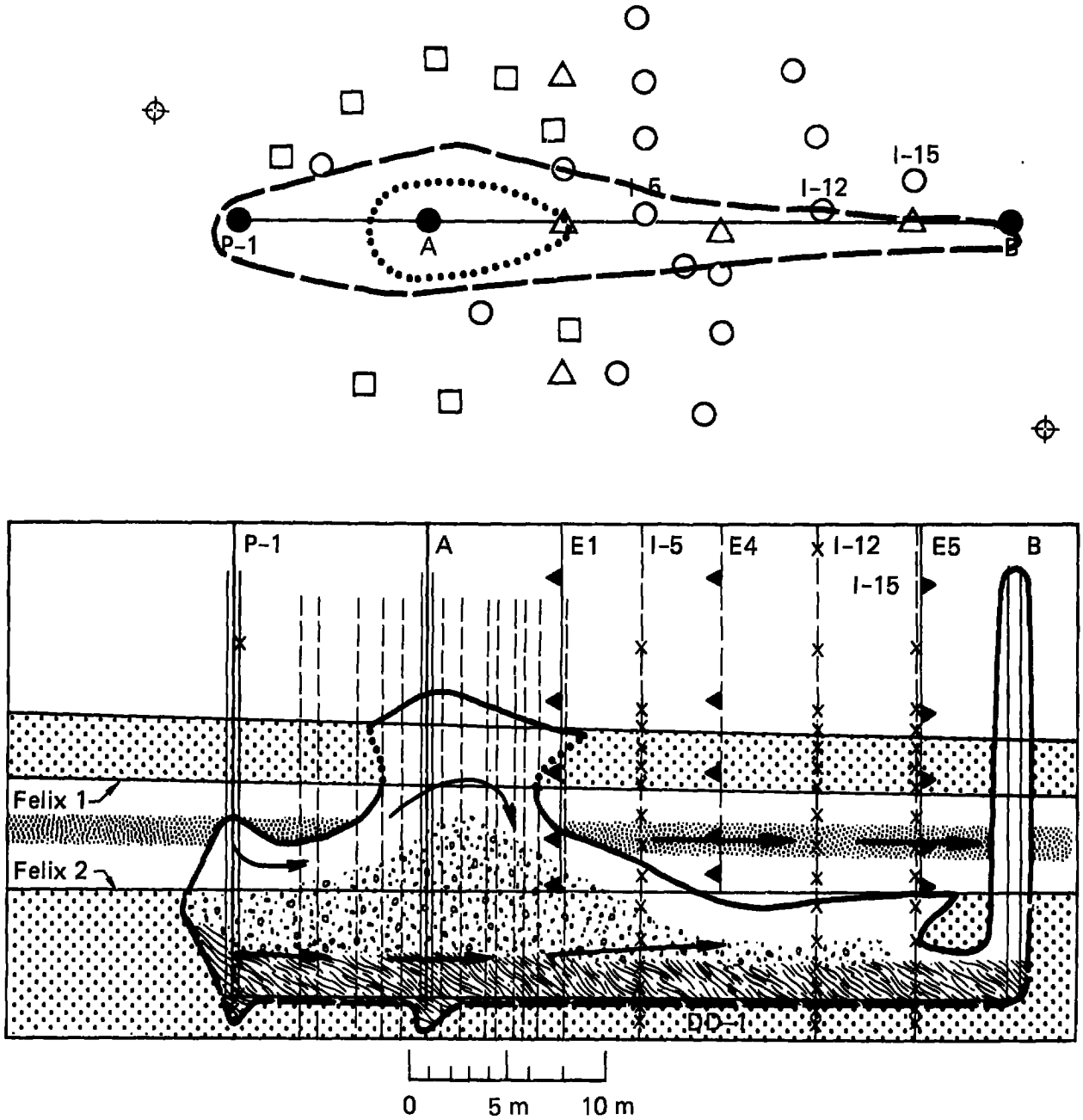


FIG. 17. Hoe Creek No. 3 burn cavity at day 242.

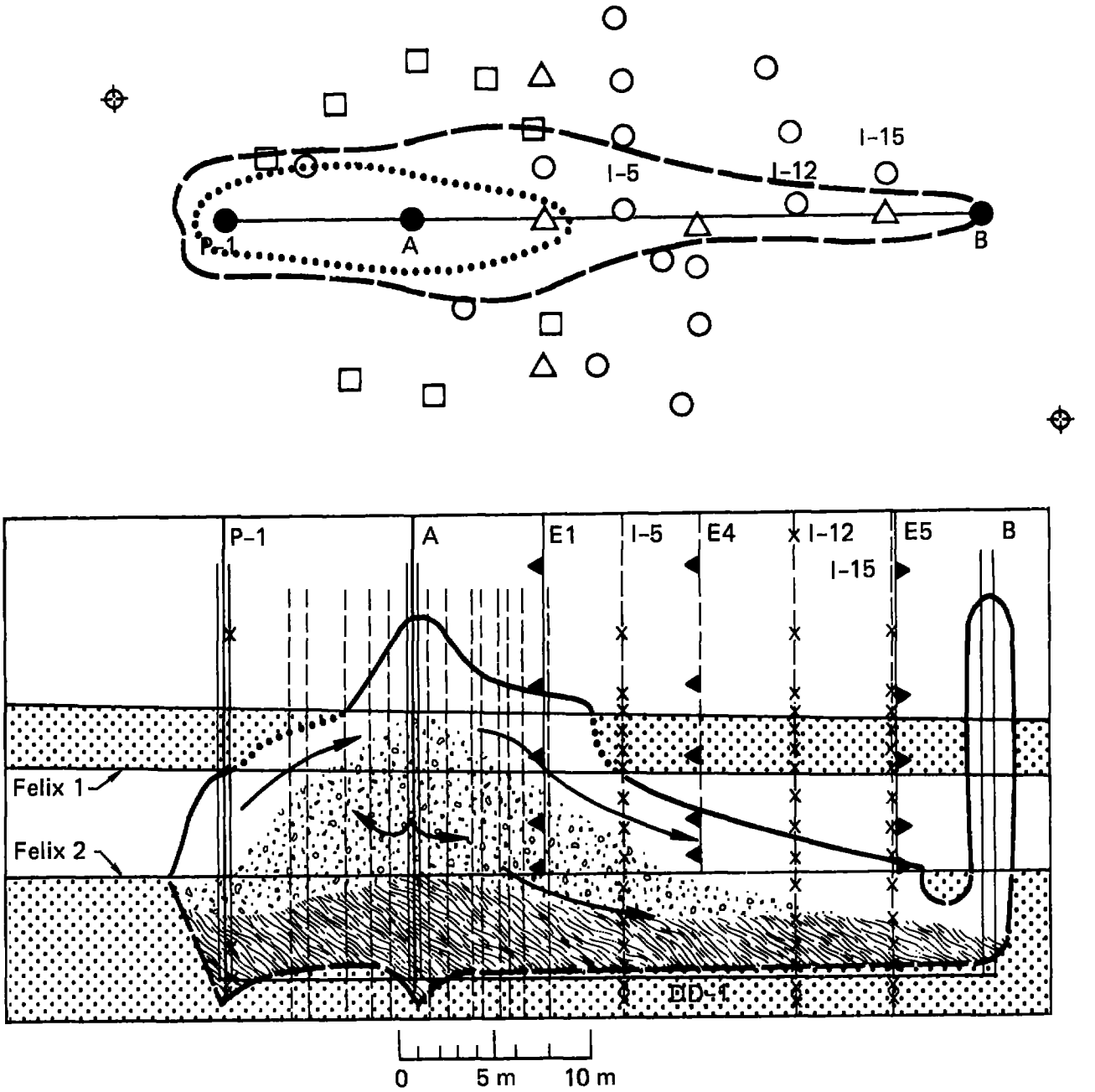


FIG. 18. Hoe Creek No. 3 burn cavity at day 245.

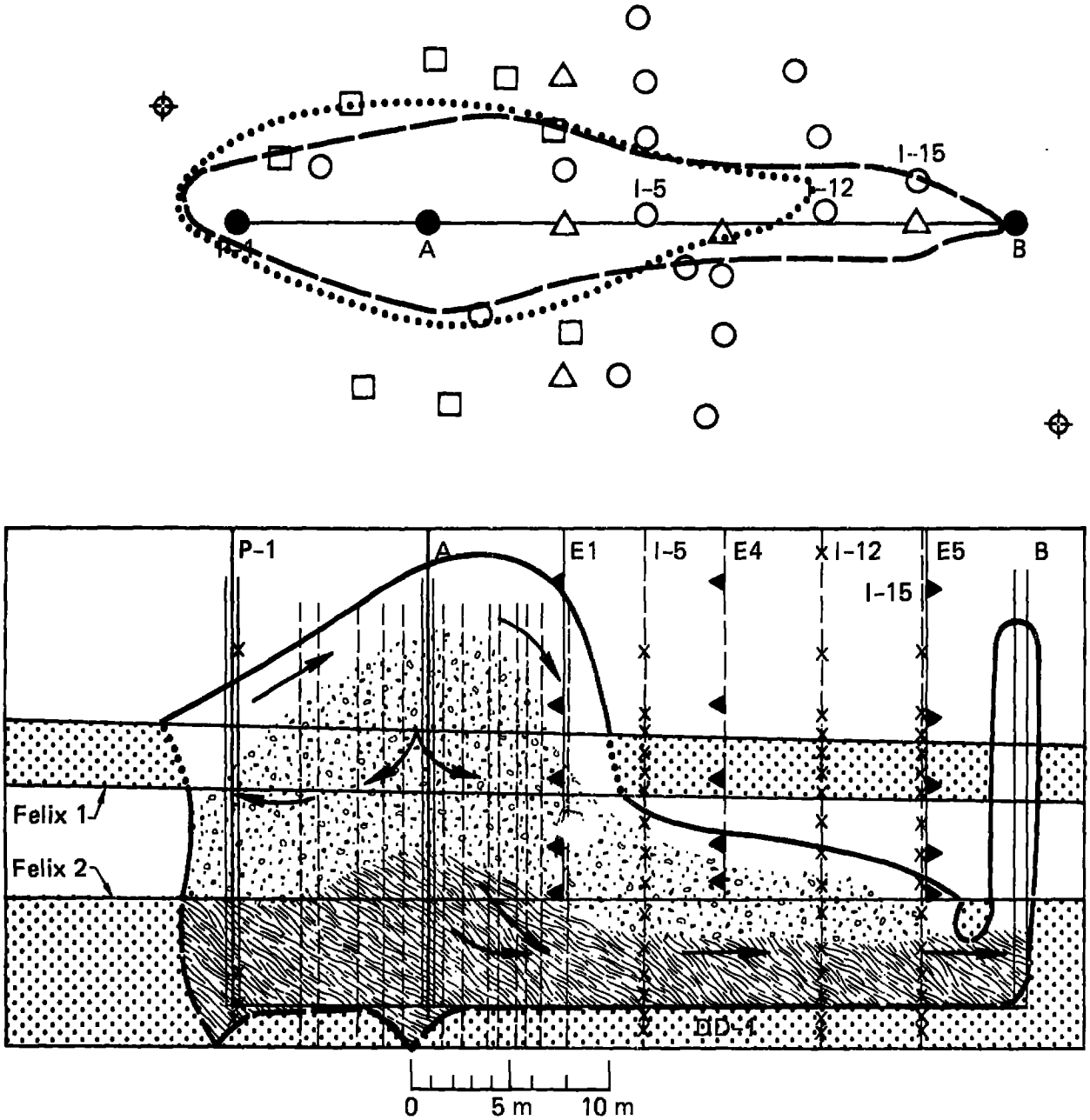


FIG. 19. Hoe Creek No. 3 burn cavity at day 248.

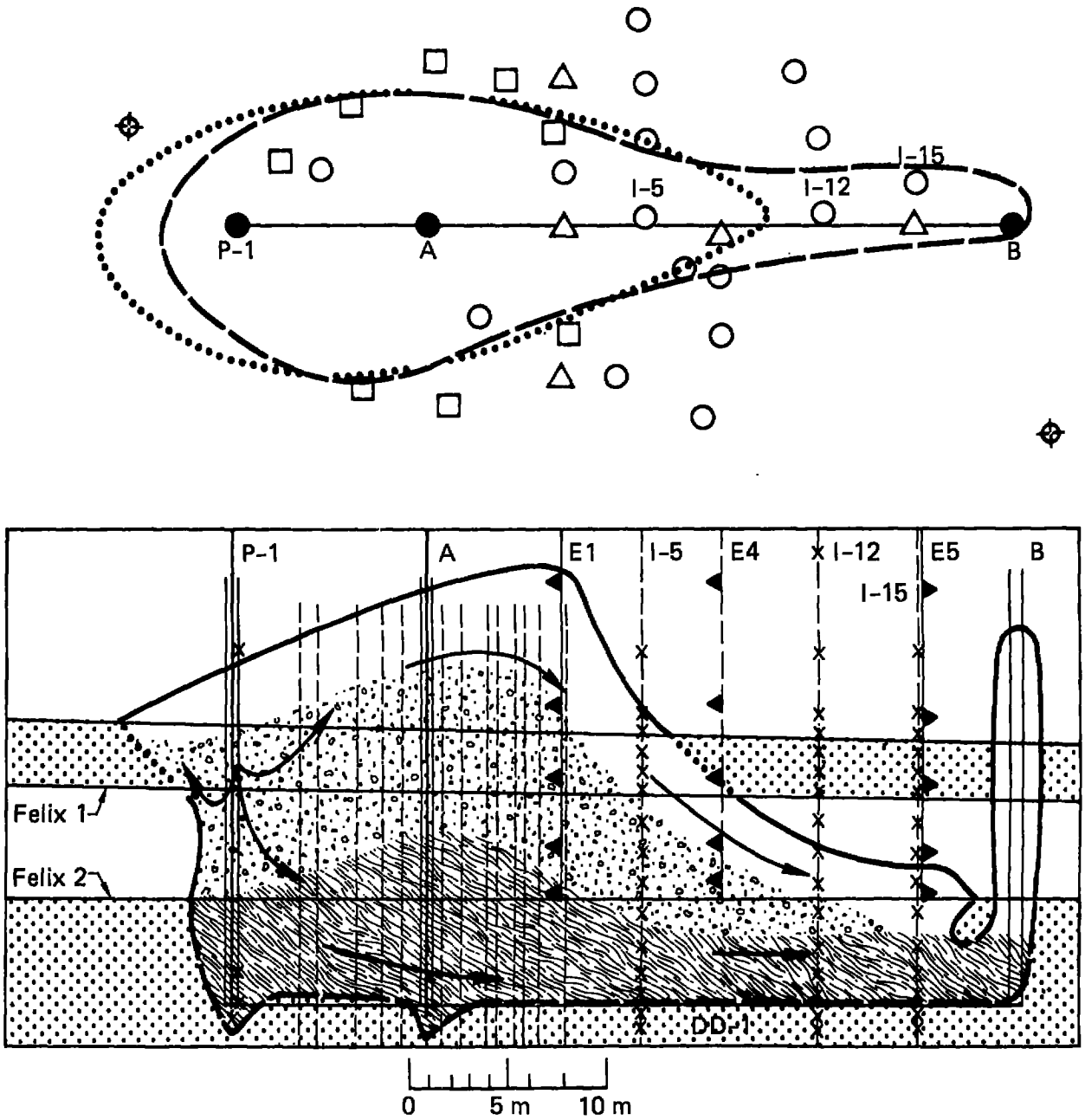


FIG. 20. Hoe Creek No. 3 burn cavity at day 252.

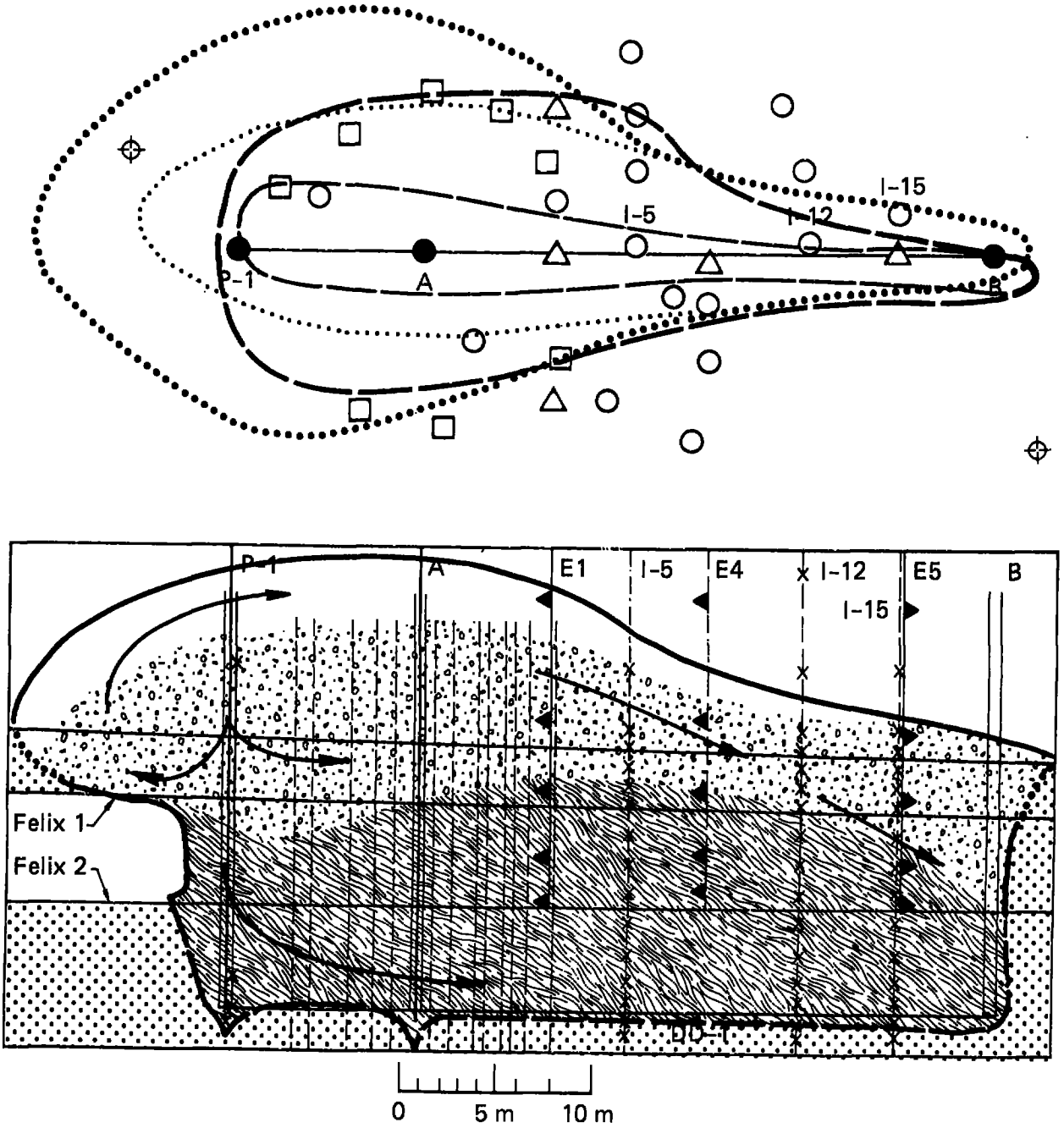


FIG. 21. Hoe Creek No. 3 burn cavity at day 282.

final constraint of the postburn coring information. An attempt has been made to show both slag and rubble formation in the cavity, but, with the exception of the final cavity, the relative amounts are mostly speculative.

Figure 22 is an artist's conception of the burn zone on day 245, based on the analysis just described. This form of presentation makes it easier to visualize the cavity.

The major points of the process history that can be correlated with these figures are:

- The product-gas heating value was high until day 233, when the burn zone reached the top of the Felix No. 2 seam. Then the heating value dropped as the parting zone collapsed into the cavity.
- The gas flowed through the drilled hole DD-1 in the Felix No. 2 seam and enlarged this linkage channel faster vertically than horizontally, but the flow was still entirely within the seam when roof collapse occurred.
- The burn progressed upward and involved the Felix No. 1 seam in less than two weeks.
- The weak roof material over Felix No. 1 collapsed into the burn zone, allowing entry of water from above.
- The final burn cavity configuration indicates that more than half of the coal consumed came from the Felix No. 1 seam.

—R. W. Hill

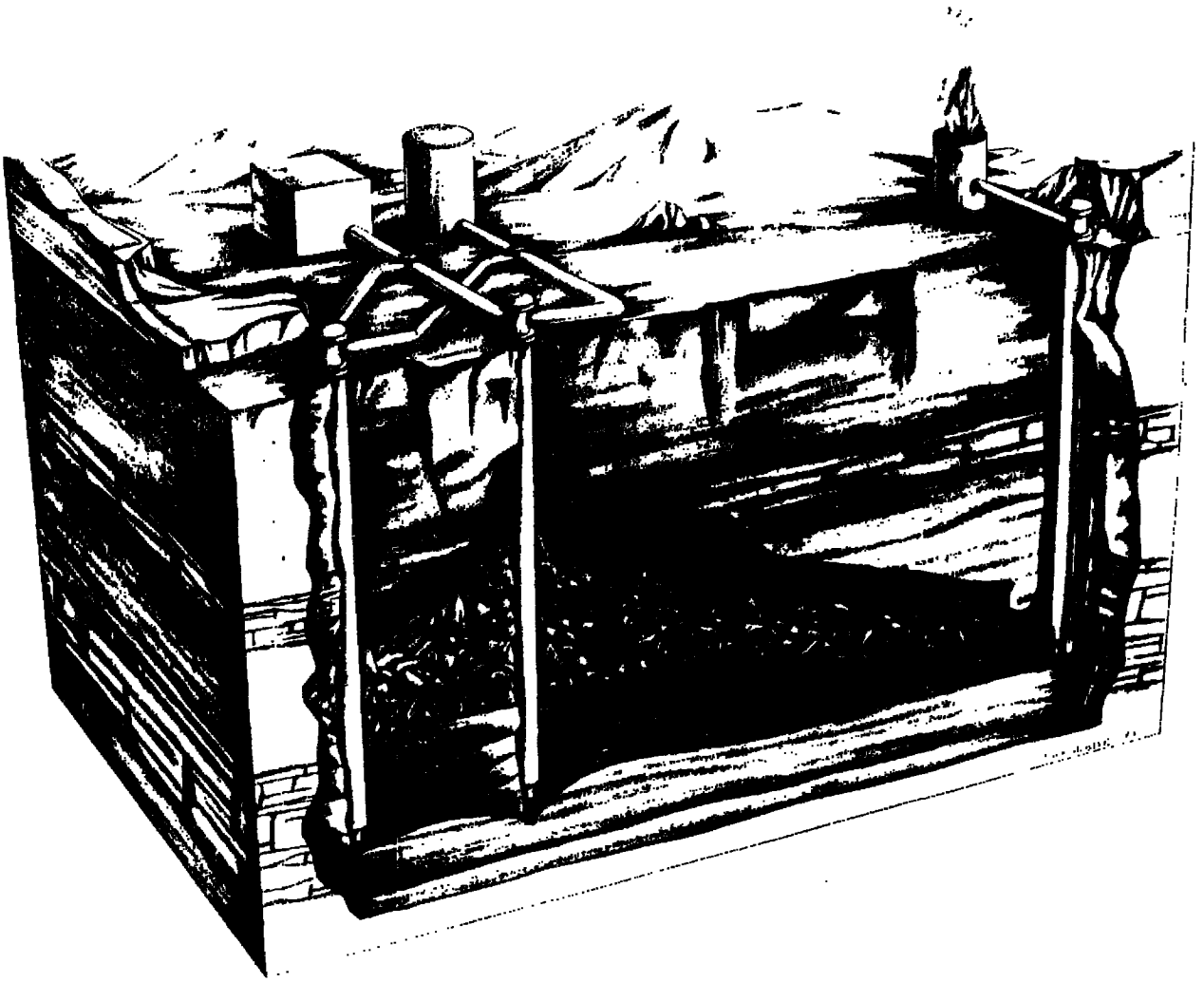

**FIG. 22. Artist's conception of Hoe Creek No. 3 burn cavity at day 245.**

# GROUNDWATER CONTAMINATION MEASUREMENTS AT HOE CREEK NO. 2

The second Hoe Creek experiment was conducted during the fall and winter of 1977, about 300 ft from the site of Hoe Creek No. 1 (Fig. 23). The Hoe Creek No. 2 experiment was considerably larger than Hoe Creek No. 1, involving the gasification of about 18 times as much coal. We had therefore hoped to compare groundwater contaminant production in the two experiments, as a first step in determining how the production of contaminants will scale with changes in the volume of gasified coal. As it turned out, roof collapse, gasification of the overlying coal, and aquifer interconnection were the major factors that affected the concentrations and distributions of the groundwater contaminants.

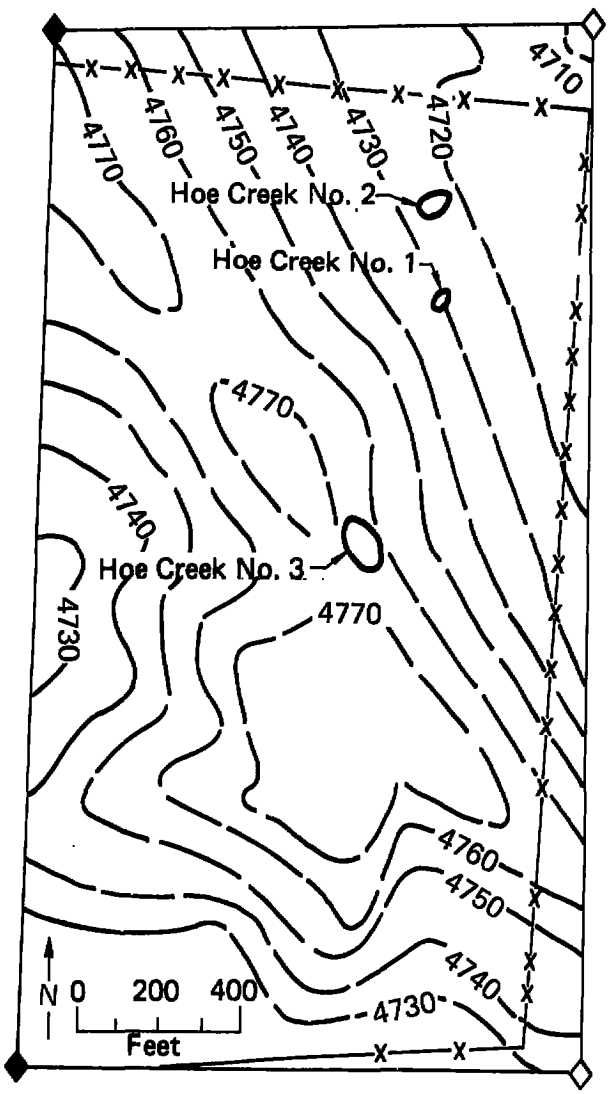


**FIG. 23. Locations of LLNL's three UCG experiments at Hoe Creek in northeastern Wyoming.**

During the site preparation stage, we constructed nine water-sampling wells, WS-1 through WS-9, in the vicinity of the Hoe Creek No. 2 experiment (Fig. 24). These wells, together with the process wells, enabled us to monitor groundwater contaminants in three regions: inside the gasification cavity (injection well A), just outside the expected cavity boundary (wells WS-2 through WS-5), and at greater distances from the gasification zone—up to 240 ft from injection well A (WS-6 through WS-9). Well WS-1 was completed in the overlying Felix No. 1 Coal within the expected gasification zone. Wells WS-5 through WS-9 were located on a line extending outward from the gasification zone in the approximate direction of natural groundwater flow (Fig. 24).

After the Hoe Creek No. 2 experiment had been completed, we recognized that additional water-sampling wells would be needed. Our subsurface geotechnical instruments, postburn coring operations (Fig. 25), and hydraulic head measurements (Fig. 26) provided convincing evidence that roof collapse and gasification of the Felix No. 1 Coal had interconnected three aquifers—the Felix No. 2 Coal, the Felix No. 1 Coal, and an overlying channel sand. Partly as a result of this geotechnical and hydrological evidence, we constructed additional wells, including seven completed in the Felix No. 1 Coal. We also plugged two existing wells to the bottom of the Felix No. 1 Coal and perforated the casing at a point near the middle of the Felix No. 1.

It is especially important to evaluate the transport of contaminants in a connected, noncoal aquifer, since natural sorption may be much less there than in a coal aquifer. We therefore completed six wells in the channel sand aquifer above the Felix No. 1.

Several wells completed in the Felix No. 1 and in the sand aquifer are located along a line corresponding roughly to the direction of natural groundwater flow. However, a few wells are located along different directions so that we can study directional variations in contaminant deposition and

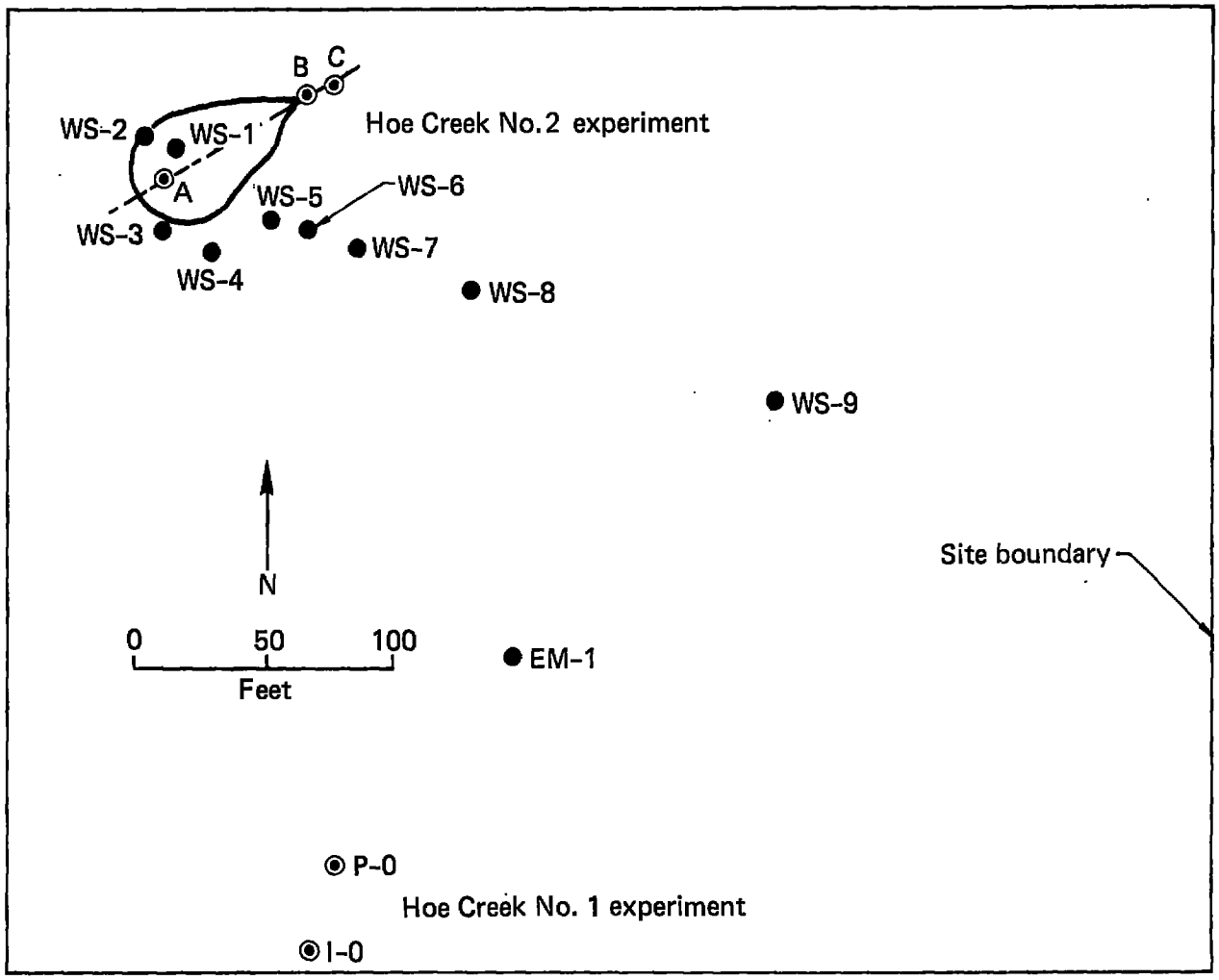


**FIG. 24. Locations of water-sampling wells in the vicinity of Hoe Creek No. 2. All wells were completed before the gasification experiment; some were destroyed in the experiment, and some were plugged after the experiment. An updated map of the wells is shown in Fig. 28.**

movement. Well WS-23, for example, is in the direction of maximum permeability. Notice that the water flow direction in the immediate vicinity of the gasification zone is, for a time, radial flow to or from the cavity, as a result of aquifer interconnection.

We believe that the array of wells now available—with, perhaps, a few additions, which may be suggested by future results—will enable us to provide reasonably complete information concerning contaminant transport away from the UCG site.

The locations of all current wells near the Hoe Creek No. 2 site are shown in Fig. 27, and additional information is supplied in Table 4. We note that three of the original wells (WS-1, WS-2, WS-3) have been plugged. They were all effectively inside the cavity and gave results that were almost identical to those obtained from injection well A. In addition, well WS-4 was reworked so as to be completed in the Felix No. 1 and was renamed WS-26.

## PREGASIFICATION RESULTS

Although the site of Hoe Creek No. 2 is only about 300 ft from the first experiment, we found that its baseline water quality was not significantly affected by the previous experiment. This is perhaps because of the short duration of the Hoe Creek No. 1 experiment.

From Table 4, we see that most wells completed in the Felix No. 1 Coal and in the sand

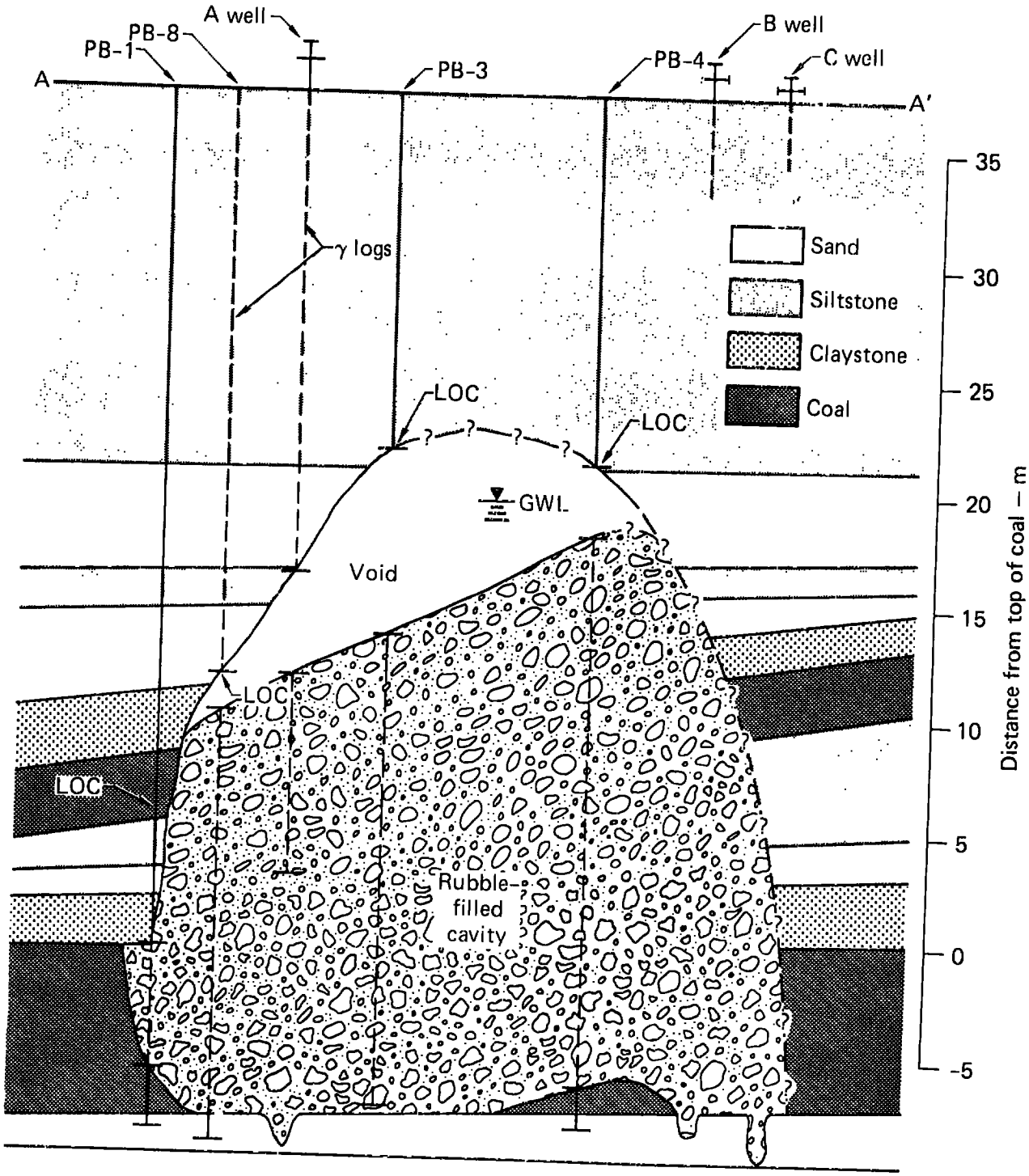


FIG. 25. Inferred shape of the Hoe Creek No. 2 gasification cavity, based on postburn coring and logging investigations. Roof collapse and resulting gasification of the overlying Felix No. 1 Coal contributed to the vertical extension of the cavity.

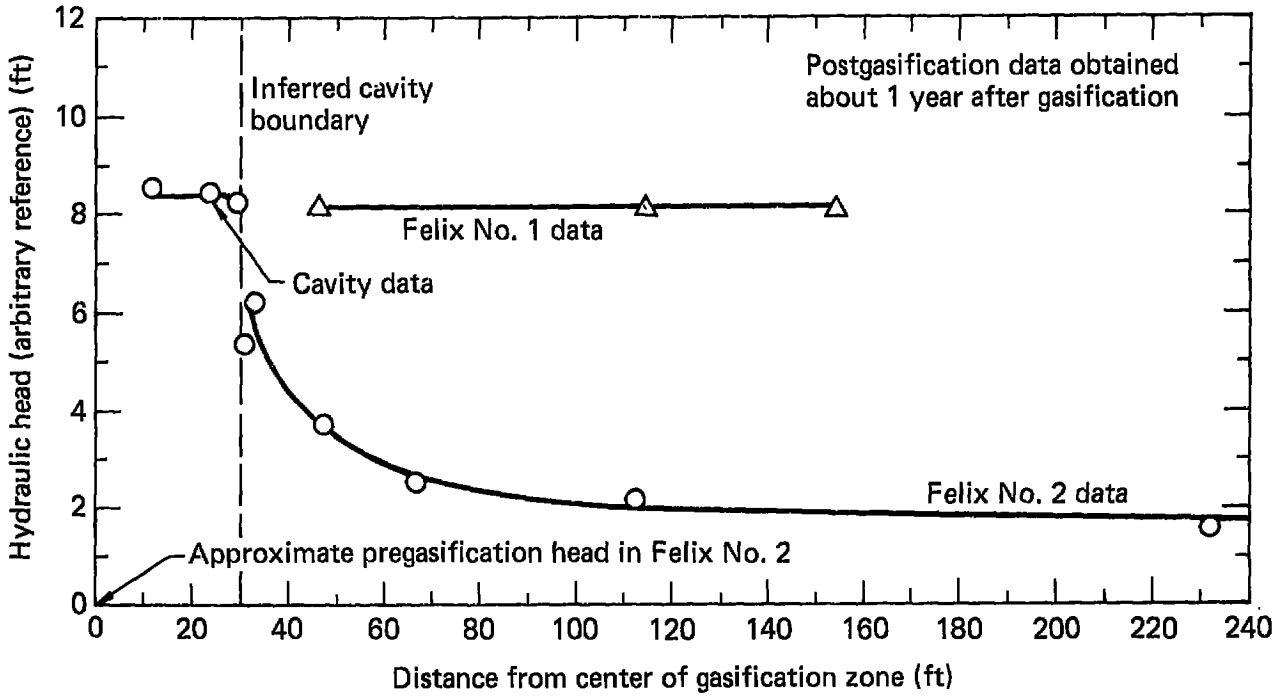


**FIG. 26. Hydraulic head data obtained near the Hoe Creek No. 2 gasification site, indicating that the Felix No. 2 Coal connected with overlying aquifers. Postgasification data were obtained about a year after gasification ended.**

aquifer were constructed after the second experiment, and therefore were not available for pregasification sampling. Well WS-1 (Fig. 24) was the only well completed in the Felix No. 1 Coal at Hoe Creek No. 2 before gasification, and no wells were completed in the sand. At the site of Hoe Creek No. 1, we had one well in the Felix No. 1 Coal (OW-12) and one well in the sand aquifer (OW-10); however, we had only limited analyses of the water samples collected from these two wells before the Hoe Creek No. 2 experiment. We have used these analyses as baseline data for these aquifers, since we believe the first experiment did not affect the Felix No. 1 Coal or the sand aquifer. The analyses are shown in Table 5.

Because of the interconnection of the three aquifers as a result of the Hoe Creek No. 2 experiment, the water inside the cavity must be a mixture of water from all aquifers. In order to understand the postburn water-quality changes, it is useful to have a comparison of the baseline data for the three aquifers. The comparison is shown in Table 5. The results indicate that the major dissolved inorganic species decrease as the location of the aquifer gets deeper.

For the water samples obtained near the Hoe Creek No. 2 experiment, we did not fractionate the dissolved organic carbon (DOC) for separate analyses, as was done at Hoe Creek No. 1, and we did not carry out methane analysis. The DOC fractionation did not offer much useful information, and for the Hoe Creek No. 2 experiment we had extensive GC-MS (i.e., gas chromatograph, mass spectrograph) analyses of the water samples. We expected that methane concentrations would be similar to those measured near the first experiment. Furthermore, methane is not likely to be a significant environmental problem, because when the groundwater is exposed to air, the methane will leave the water.

## RESULTS DURING GASIFICATION

Since dewatering was not employed for the Hoe Creek No. 2 experiment, it was necessary to use higher system pressures—above the hydrostatic pressure—to limit the amount of groundwater entering the cavity during gasification. The higher gas pressures pushed the groundwater quite far away

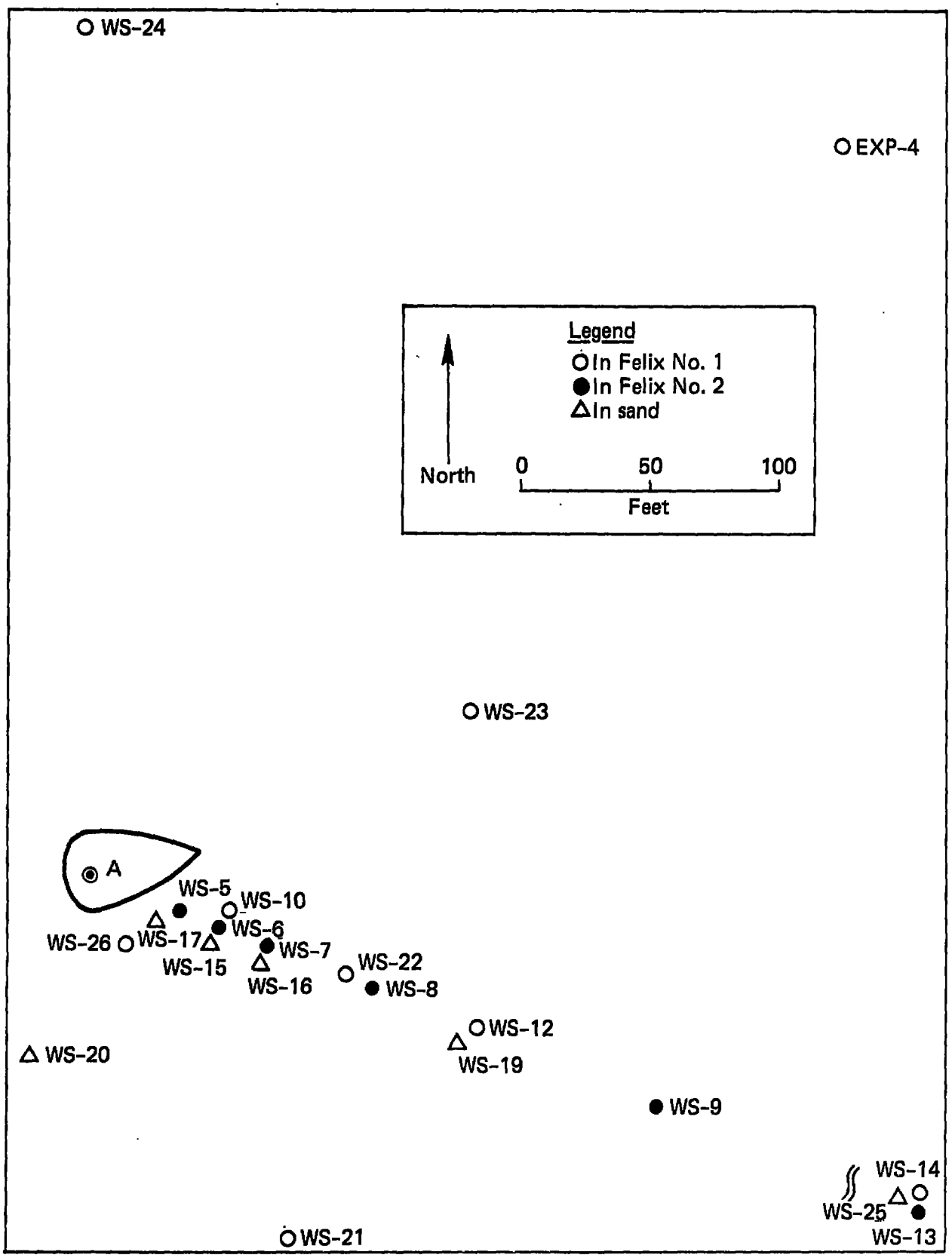


**FIG. 27. Locations of all current water-sampling wells in the vicinity of Hoe Creek No. 2.**

TABLE 4. **Information on water wells at the Hoe Creek No. 2 site. All distances and bearings were measured with respect to the injection well A.**

| Well | Distance (ft) | Bearing | Date of completion | Aquifer |
|---|---|---|---|---|
| A | 0 | 0 | Pregasification | Inside cavity |
| WS-5 | 39 | S 68° 4'14" E | " | Felix No.2 |
| WS-6 | 55 | S 67° 56'32" E | " | " |
| WS-7 | 75 | S 68° 5'32" E | " | " |
| WS-8 | 120 | S 68° 13'32"E | " | " |
| WS-9 | 239 | S 68° 25'44" E | " | " |
| WS-10 | 55 | S 76° 25'44" E | Nov. 1978 | Felix No. 1 |
| WS-12 | 163 | S 68° 43'32" E | " | " |
| WS-13 | 403 | S 68° 17'26" E | Jun. 1979 | Felix No. 2 |
| WS-14 | 400 | S 69° 24'8" E | " | Felix No. 1 |
| WS-15 | 56 | S 60° 20'44" E | Feb. 1980 | Sand |
| WS-16 | 76 | S 60° 34'32" E | " | " |
| WS-17 | 32 | S 54° 42'26" E | " | " |
| WS-19 | 160 | S 65° 55'26" E | Oct. 1980 | " |
| WS-20 | 75 | S 16° 49'22" W | " | " |
| WS-21 | 162 | S 29° 25'20" E | " | Felix No. 1 |
| WS-22 | 108 | S 68° 33'8" E | " | " |
| WS-23 | 161 | N 66° 9'44" E | " | " |
| WS-24 | 331 | N 1° 12'38" E | " | " |
| WS-25 | 395 | S 68° 50'47" E | " | Sand |
| WS-26 | 30 | S 27° 58'44" E | " | Felix No. 1 |
| Exp-4 | 408 | N 45° 37'34" E | " | " |

TABLE 5. **A comparison of groundwater baseline data for the three aquifers.**

| | Aquifer | | |
|---|---|---|---|
| | Felix No. 2 | Felix No. 1 | Sand |
| Electrical conductivity (μmho/cm) | 1080 ± 150 | 2070 | 2700 |
| pH | 7.5 ± 0.1 | 7.1 | 7.7 |
| Temperature (°C) | 11.0 ± 3 | 10.5 | 10.0 |
| Alkalinity (ppm) | 401 ± 33 | 260 | 270 |
| Ammonium (ppm) | 0.7 | 0.5 | 1.4 |
| Boron (ppb) | 86 ± 30 | 50 | 80 |
| Calcium (ppm) | 36 ± 10 | 190 | 270 |
| Chloride (ppm) | 13 ± 5 | 8 | 9.3 |
| Cyanide (ppb) | 0–2 | 0 | 0 |
| Magnesium (ppm) | 10 ± 4 | 73 | 67 |
| Phenols (ppb) | 0–2 | 1 | — |
| Potassium (ppm) | 5.4 ± 0.5 | 8 | 16 |
| Sodium (ppm) | 214 ± 15 | 190 | 320 |
| Sulfate (ppm) | 154 ± 80 | 800 | 1300 |

from the cavity, so that most water-sampling wells were dry during gasification. Therefore, we had very limited sampling opportunities during gasification. Wells WS-2, WS-7, and WS-9 were sampled, and a water sample from WS-2 was analyzed by GC-MS. The results are shown in Tables 6 and 7.

The water collected from WS-2 during gasification (Fig. 24) must have come from quite close to the burn front, because 20 days later when the operation was shut down, the casing and pump were found to have been destroyed and the well was, by then, inside the cavity.

We were not surprised to find that pyrolysis products (phenols, cyanide, etc.) were detected in WS-9 (240 ft from the injection well A) during gasification and that a significant increase occurred in the concentrations of $Ca^{2+}$, $Mg^{2+}$, $K^{+}$, and $Na^{+}$, and in the electrical conductivity. We had observed similar phenomena in the first experiment. (An explanation of the increase of $Ca^{2+}$, etc., will be discussed in connection with Hoe Creek No. 3.) We are

TABLE 6. Analysis of groundwater samples collected during the Hoe Creek No. 2 experiment, and comparison with baseline data.

| | Well WS-7 | | Well WS-9 | |
|---|---|---|---|---|
| | During | Baseline | During | Baseline |
| Electrical conductivity (μmho/cm) | 3200 | 1130 | 1700 | 1080 |
| pH | 6.5 | 7.2 | 6.3 | 7.0 |
| Temperature (°C) | 11 | 11.4 | 12.0 | 12 |
| Alkalinity (ppm) | 1480 | 312 | 1120 | 490 |
| Ammonium (ppm) | 2.3 | 0.8 | 1.2 | 0.6 |
| Boron (ppb) | 140 | 60 | 110 | 60 |
| Calcium (ppm) | 180 | 51 | 100 | 31 |
| Chloride (ppm) | 7.0 | 6.9 | 7.3 | 7.8 |
| $CO_2$ (ppm) | 916 | 38 | 1090 | 100 |
| Cyanide (ppb) | 20 | 0 | 0 | 0 |
| Magnesium (ppm) | 49 | 12 | 35 | 7.2 |
| Phenols (ppb) | 860 | 2 | 45 | 2 |
| Potassium (ppm) | 9.4 | 4.9 | 6.4 | 3.9 |
| Sodium (ppm) | 560 | 270 | 360 | 230 |
| Sulfate (ppm) | 120 | 300 | 22 | 110 |
| Sulfide (ppm) | 1.9 | 2.0 | 3.8 | 0.6 |
| DOC (ppm) | 26.5 | 3.2 | 9.9 | — |

puzzled, however, by the decrease in sulfate concentration, and we do not have a satisfactory explanation for it. Perhaps the sulfate was reduced by chemicals that come from pyrolysis. We did analyze for sulfate-reducing bacteria in the groundwater, with negative results.

## POSTGASIFICATION RESULTS

During the Hoe Creek No. 2 experiment, the groundwater hydraulic heads were affected out to at least several hundred feet from the cavity; wells out to about 100 ft were dry. Following gasification, the groundwater, which has been at least partially excluded from the cavity by gas pressure, returns to the cavity and, for a few weeks, is partially vented in the form of steam. The cavity will have largely refilled with water in a month or so, and the hydraulic heads inside and outside the cavity will gradually reach equilibrium. Since this is an area of natural recharge to groundwater, and because of the interconnection of aquifers, the hydraulic head inside the cavity is higher than the head in the Felix No. 2 Coal (Fig. 24).

It is convenient to discuss the groundwater contamination at the site of the Hoe Creek No. 2 experiment in terms of the effects in four regions: the gasification cavity, the Felix No. 2 Coal aquifer, the Felix No. 1 Coal aquifer, and the sand aquifer.

### The Gasification Cavity

Groundwater quality within the cavity is affected by the returning water and the natural groundwater flow in two ways. Inorganic materials are slowly leached from the pile of ash and rubble, and certain soluble pyrolysis products, initially deposited outside the cavity, are swept into the cavity—especially such water-soluble products as ammonia. These two sources may continue to introduce contaminants into the cavity for a matter of years. Figure 28 illustrates the persistence, within the Hoe Creek No. 2 cavity, of some contaminants that may be of importance. The contaminant species plotted in Fig. 28—ammonium, fluoride, and boron (as borates)—are examples of cavity contaminants that increase significantly after gasification and persist in the cavity groundwater. Other such species include total sulfide, chloride, and

TABLE 7. A GC/MS analysis of groundwater sample collected from WS-2 during gasification.

| Compound | Concentration (ppb) | Compound | Concentration (ppb) |
|---|---|---|---|
| Methylcyclopentene isomer (tentative) | NQ | Trimethylbenzene isomer | ~14 000 |
| Benzene | >20 000 | n-decane | >20 000 |
| 1,2-dibromoethane | IS | Trimethylbenzene isomer | ~16 000 |
| n-hexane | >20 000 | $C_9H_{10}$ isomer (tentative) | NQ |
| Dimethylcyclopentene isomer (tentative) | NQ | n-undecane | >20 000 |
| $C_7H_{12}$ isomer (tentative) | NQ | $C_{10}H_{12}$ isomer (tentative) | NQ |
| Methylthiophene isomer | ~1 800 | $C_{10}H_{12}$ isomer (tentative) | NQ |
| $C_8H_{14}$ isomer (tentative) | NQ | $C_4$ alkylbenzene isomer | ~14 000 |
| Methylthiophene isomer | ~7 500 | Naphthalene | >20 000 |
| $C_7H_{12}$ isomer (tentative) | NQ | $C_{11}H_{14}$ isomer (tentative) | NQ |
| Noise spike | — | $C_{11}H_{14}$ isomer (tentative) | NQ |
| $C_8H_{14}$ isomer (tentative) | NQ | n-dodecane | >20 000 |
| Toluene | >20 000 | $C_{13}$ alkane | ~13 000 |
| Noise spike | — | $C_{11}H_{14}$ isomer (tentative) | NQ |
| Ethylbenzene | >20 000 | Methylnaphthalene isomer | >20 000 |
| Column artifact | — | n-tridecane | >20 000 |
| $C_8H_{18}$ isomer | >20 000 | $C_{12}H_{16}$ isomer (tentative) | NQ |
| m- and/or p-xylene | >20 000 | $C_{13}H_{18}$ isomer (tentative) | NQ |
| o-xylene | >20 000 | $C_{14}$ alkane | ~16 000 |
| n-propylbenzene | >17 000 | n-tetradecane | >20 000 |
| o-methylstyrene (tentative) | NQ | $C_{15}$ alkane | ~15 000 |
| $C_9H_{12}$ isomer | >20 000 | n-pentadecane | >20 000 |
| o-ethyltoluene | >20 000 | Trimethylnaphthalene isomer | ~8 500 |
| n-nonane | >20 000 | Dimethyl phthalate (tentative) | AS |
| $C_{10}H_{14}$ isomer | >20 000 | n-hexadecane | >20 000 |
| $C_{10}H_{14}$ isomer | >20 000 | $C_{17}$ alkane | ~9 000 |
| $C_{10}H_{12}$ isomer (tentative) | NQ | n-heptadecane | >20 000 |
| Noise spike | — | $C_{18}$ alkane | ~9 200 |
| $C_9H_{12}$ isomer | >20 000 | $C_{18}$ alkene | ~10 000 |
| Trimethylbenzene isomer | >20 000 | D-10 anthracene | IS |
| $C_9H_{12}$ isomer | ~5 000 | n-octadecane | 11 000 |
| $C_9H_{12}$ isomer | >20 000 | n-nonadecane | 9 500 |
| Phenol | >20 000 | n-eicosane | 7 400 |
| o-cresol | >20 000 | n-heneicosane | 8 200 |
| p-cresol | >20 000 | n-docosane | 7 600 |
| Dimethylphenol isomer | ~8 200 | n-tricosane | 8 300 |
| $C_2$ alkylphenol isomer | >20 000 | n-tetracosane | 8 400 |
| $C_3$ alkylbenzene isomer | ~14 000 | n-pentacosane | 8 500 |
| $C_3$ alkylbenzene isomer | ~12 000 | n-hexacosane | 4 400 |
| | | n-heptacosane | ~4 700 |

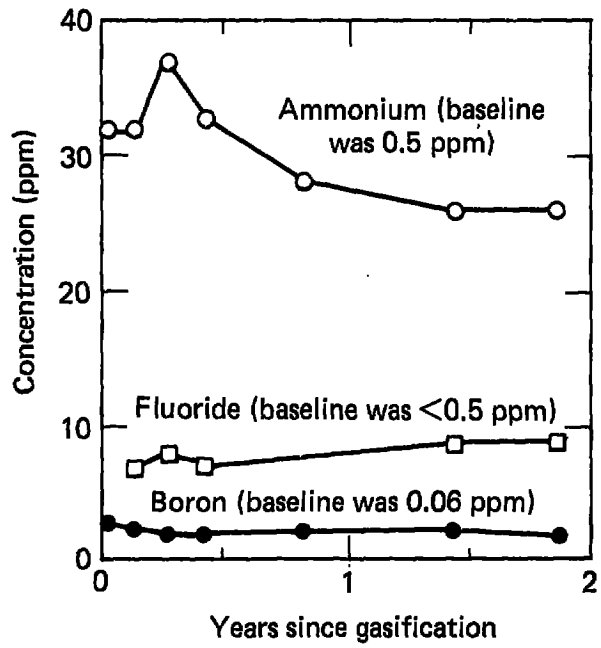


**FIG. 28. Changes in concentration of important contaminants with time for goundwater inside the Hoe Creek No. 2 cavity.**

silicon (as silicates). Another class of contaminants comprises those that appear in significant concentrations within the cavity after gasification, but show a gradual decrease as a result of sorption, dilution, or chemical reactions. These materials include phenols, sulfate, calcium, magnesium, potassium, and lithium. Slightly different behavior was exhibited by arsenic, which showed a small increase in the Hoe Creek No. 2 cavity after gasification (0.010 ppm) and then returned to its pregasification level (0.002 ppm) after 10 months.

Our laboratory studies have shown that the major inorganic species from the leaching of coal ash are sulfate and calcium. The changes of sulfate and calcium inside the Hoe Creek No. 1 cavity agreed well with the laboratory results. Initial concentrations, after gasification, were higher than baseline values and kept increasing as a result of continued leaching of the coal ash. Then, after reaching a maximum, these concentrations began to decrease due to dispersion and dilution. In contrast to this behavior, changes in sulfate and calcium inside the Hoe Creek No. 2 cavity have constantly decreased (Fig. 29). Even the initial postgasification concentrations of sulfate and calcium were comparatively low (950 ppm and 140 ppm) in view of the relatively high baseline values in the sand and in the Felix No. 1 Coal (Table 5). After two years, the concentrations of sulfate and calcium inside the Hoe Creek No. 2 cavity are below the baseline values of the Felix No. 2 Coal aquifer—the lowest values among the three aquifers. One might think that the low concentrations of these species in the Hoe Creek No. 2 cavity are a result of sorption by the siltstone and claystone that fell into the cavity during roof collapse. This explanation is not fully satisfactory, however, because, as we shall see, the decrease in sulfate and calcium is also apparent in water collected from the coal aquifers at points outside the cavity.

Evidently, the groundwater chemistry inside the Hoe Creek No. 2 cavity is very complex, and not yet fully understood. It involves the water from three aquifers, coal ash, overburden materials, and pyrolysis products. It may even involve the flow of groundwater inside the cavity (i.e., the flow from the upper to the lower aquifer in this recharge area). For example, in Fig. 28, the ammonium concentration inside the cavity remains essentially unchanged. Perhaps the water flow from the sand and the Felix No. 1 Coal to the Felix No. 2 Coal is primarily

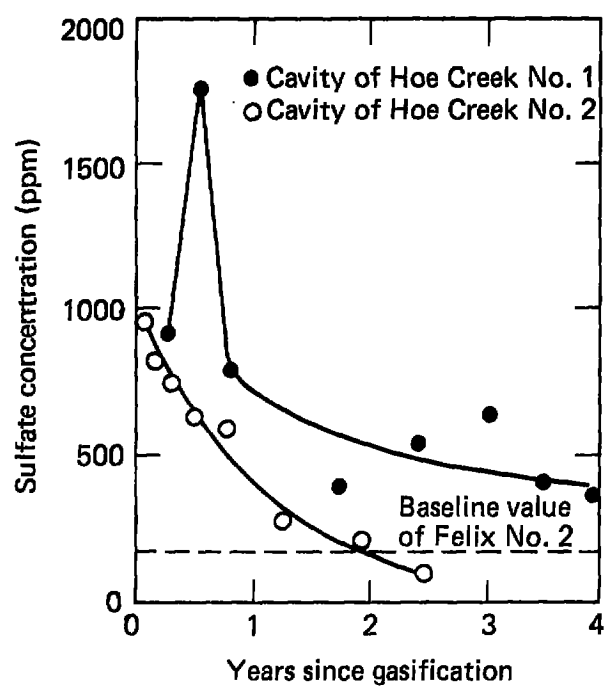


**FIG. 29. Comparison of change in sulfate concentration with time in groundwater in the cavities of Hoe Creek No. 1 and No. 2.**

along the outer edge of the cavity, with the bulk of the water inside the cavity not moving. This possibility may be very important in connection with attempts to identify an effective control technology. It may help to determine an optimum time to initiate cavity cleanup, as well as the preferred cleanup mechanism.

**The Felix No. 2 Coal Aquifer**

Contaminants in the groundwater outside the cavity come from two sources—pyrolysis products, and leachates from the coal ash. The pyrolysis products are initially deposited outside the cavity. They are dissolved and, to some extent, moved inward by the returning groundwater, and then subsequently swept outward again when the groundwater begins to move away from the cavity. Another group of contaminants—most of the inorganics—is introduced into the groundwater from the ash within the cavity, and later transported outward into the surrounding coal. Boron is an interesting example of the internally deposited contaminants; our laboratory studies indicate that it is only weakly sorbed by the surrounding coal, and it is toxic for some plants at concentrations above 1 ppm. Furthermore, as we have indicated, it may occur as a persistent source within the cavity.

It seems clear that the interconnection of the three aquifers has had a significant influence on groundwater flow rates and contaminant movement near the gasification zone. This is especially true in the Felix No. 2 Coal aquifer, for which the normal groundwater flow is replaced, locally, by a radial flow away from the cavity. The effect of this increased flow on contaminant movement is suggested by comparing boron transport in Felix No. 2 at Hoe Creek No. 2 with its movement at the Hoe Creek No. 1 site. The movement of boron away from Hoe Creek No. 2 is illustrated in Fig. 30. At the Hoe Creek No. 1 site, we have measured increased boron concentrations in wells that are approximately 10 ft from the cavity boundary; after

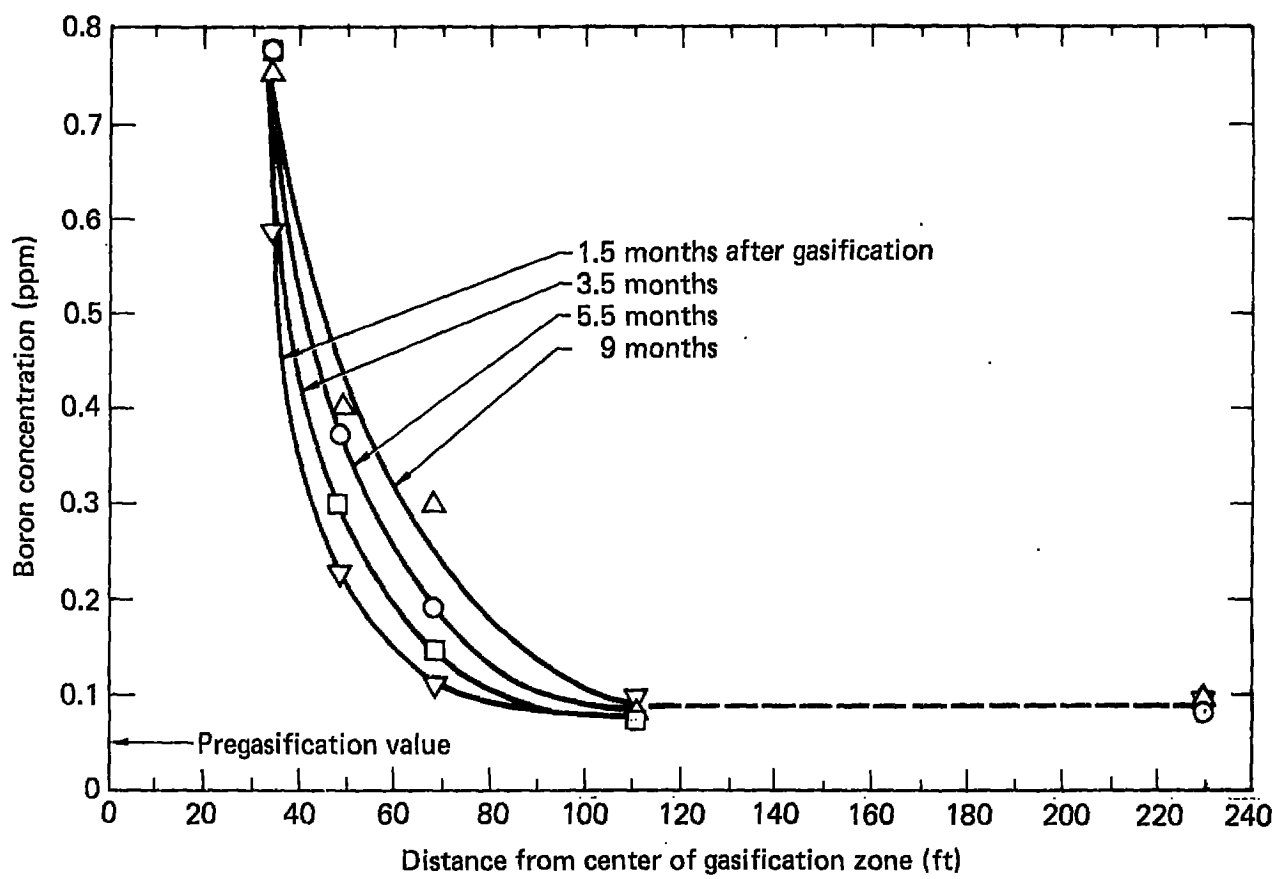


**FIG. 30. Changes in boron concentration in groundwater with distance from the Hoe Creek No. 2 site. Water was taken from WS-5 (about 40 ft from the center of the cavity), WS-6 (~50 ft), WS-7 (~70 ft), WS-8 (~110 ft), and WS-9 (~230 ft).**

nearly four years, however, we have not detected boron in any of the more distant wells, the closest of which is about 40 ft from the cavity. At Hoe Creek No. 2, where aquifer interconnection produced additional groundwater flow, we measure a definite increase in boron concentration at well WS-7 (roughly 30 ft from the cavity boundary, see Fig. 30) less than six months after gasification. Some recent boron measurements at Hoe Creek No. 2 are shown in Fig. 31, which indicates that, although boron levels may be decreasing in the close-in well WS-5, they are remaining nearly constant in WS-7, almost two and a half years after gasification. We note, however, that boron increases have not been detected in any of the more distant wells, and that the concentrations measured outside the cavity are generally well below the 1-ppm level. The increased groundwater flow resulting from aquifer interconnection seems to have much less effect on contaminant movement at distances of 100 ft or more from the cavity.

Since water flows quickly from the cavity into the nearby wells completed in the Felix No. 2 Coal, we would expect to see changes in the sulfate and calcium concentrations similar to those measured inside the cavity—that is, continuously decreasing. More distant wells might, of course, show different changes in sulfate and calcium concentrations. A comparison of sulfate changes in WS-5 and WS-9 is shown in Fig. 32. Again, we do not understand why the concentration of sulfate in WS-9 is much lower, after gasification, than the baseline value. Well WS-13 is located 403 ft from the injection well A. It was constructed about two and a half years after gasification. The water quality has been similar to the baseline data, except that the sulfate concentration is lower. Our best guess is that the sulfate was originally lower in that region, and that the water in WS-13 has not yet (after three years) been affected by the gasification.

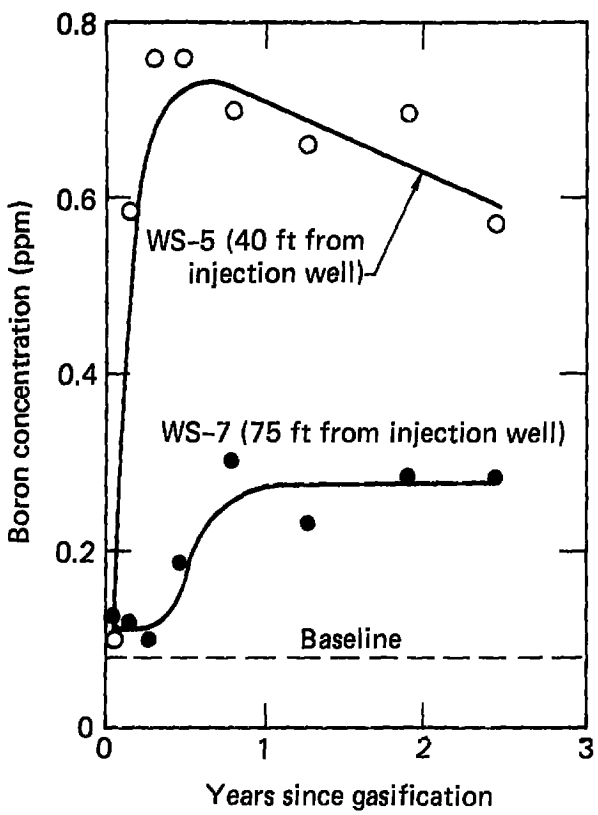


**FIG. 31. Change in boron concentration in the groundwater in the Felix No. 2 Coal aquifer as a function of time since the Hoe Creek No. 2 experiment.**

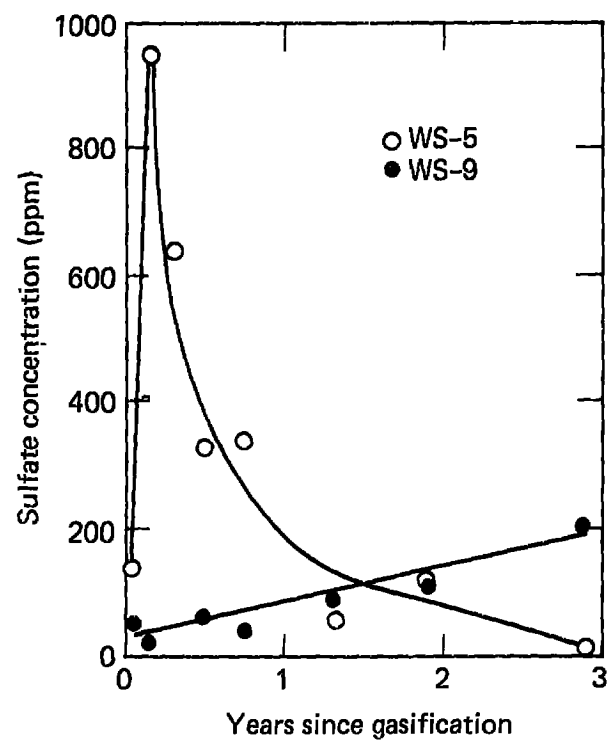


**FIG. 32. Comparison of the change in sulfate concentration with time for wells WS-5 (39 ft from injection well A) and WS-9 (239 ft from well A). The initial sulfate increase in WS-5 is due to water flow into the well from the cavity. The baseline value of sulfate in the groundwater in the Felix No. 2 Coal aquifer is approximately 200 ppm.**

Our groundwater measurements after the Hoe Creek No. 1 experiment indicated that the quantity of deposited organic pyrolysis products depends sensitively on distance from the cavity boundary (Fig. 33 uses phenols as an example). This leads us to believe that, under the conditions existing at Hoe Creek No. 1, the organic contaminants are deposited primarily near the edge of the cavity. For the second experiment, however, the strong variations in the concentrations of organic materials as a function of distance are less apparent. This may be, in part, because we do not have a well completed in the Felix No. 2 Coal at Hoe Creek No. 2 that is really close to the cavity boundary (within a foot or two). In any case, we have not found very high concentrations of any organic contaminant in the Felix No. 2 at Hoe Creek No. 2. The highest phenol concentration was 7 ppm in WS-5, 52 days after gasification. We have detected volatile organics shortly after gasification, at large distances from the gasification cavity, at low but measurable concentrations. For example, toluene was found at a concentration of approximately 0.1 ppm in well WS-9 (Fig. 24 and Table 4), nearly 200 ft from the burn zone, two weeks after gasification. A more detailed discussion of the organic contaminants introduced into the groundwater as a result of UCG is presented in a later section of this report.

Another interesting difference in the water quality results at Hoe Creek No. 1 and No. 2 is related to the changing concentrations of volatile organic contaminants, such as phenols, in the groundwater at the more distant wells completed in the Felix No. 2 Coal. Well EM-1 (completed prior to Hoe Creek No. 1, 100 ft from the cavity) had phenol concentrations of 0.015 ppm three days after gasification and returned to baseline levels (0.002 ppm) after three months. Well WS-9 (Hoe Creek No. 2, 200 ft from the cavity) showed phenol concentrations of 0.032 ppm two months after gasification and has remained at 0.010 ppm (five times the baseline value) for more than two years. A plot showing the changing phenol concentrations for the two original outermost wells in the vicinity of Hoe Creek No. 2 is shown in Fig. 34.

We have considered several mechanisms that may account for the unexpected persistence of phenols and some of the other organic contaminants. In the first place, the pyrolysis products may be produced or deposited in a form that retards dissolution—perhaps in combination with sparingly soluble tars. In this case, a long-lived source would be produced that could, in part, account for our observations. We are also exploring the possibility that some form of saturation is limiting continued sorption of certain contaminants. The surfaces of the

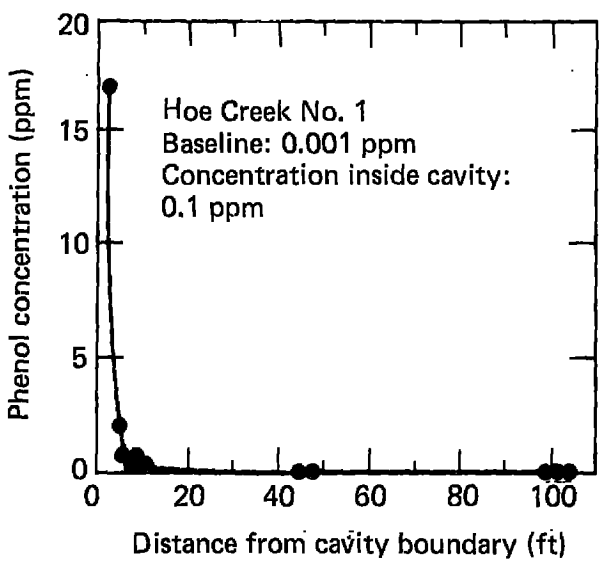


**FIG. 33. Phenol concentrations in groundwater as a function of distance from the Hoe Creek No. 1 cavity. Data were obtained three months after gasification.**

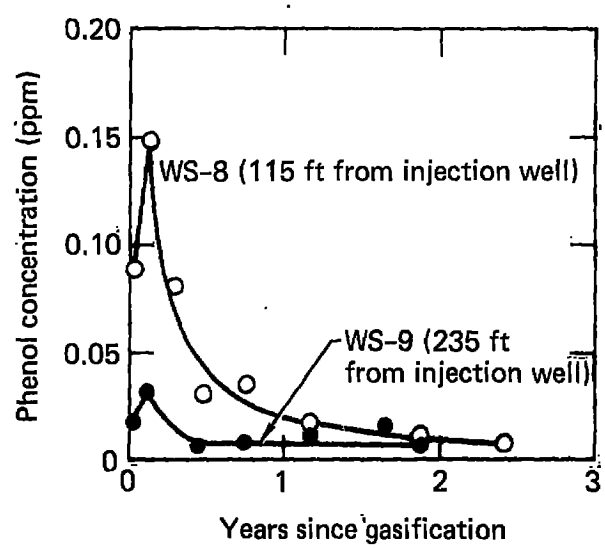


**FIG. 34. Change in phenol concentration in the Felix No. 2 Coal aquifer with time since the Hoe Creek No. 2 experiment. The most recent measurements are several times the baseline values, and about three times the lower limit of detection for these analyses.**

rubbled coal near Hoe Creek No. 1 may have simply become saturated with phenols after about a year, so that subsequent sorption has been much less effective (Fig. 35). In the case of a large, prolonged gasification operation, it may be that the volatile organics escaping into the coal during gasification are condensed or sorbed onto the coal surfaces in such a way as to restrict the coal's capacity for subsequent sorption of contaminants from the groundwater. If the outward movement of gases and groundwater through the surrounding coal is concentrated in a comparatively few large cracks (a lower surface-to-volume ratio), the possibility of saturation effects would be exaggerated. There has been some indication that large cracks or, perhaps, narrow fracture zones in the coal may have influenced contaminant transport at Hoe Creek.

**The Felix No. 1 Coal Aquifer**

There are now nine water-sampling wells completed in the Felix No. 1 Coal at the site of the Hoe Creek No. 2 experiment (Fig. 27). Most of them were constructed in October 1980, so the results of water quality analyses for these wells are not yet available. The following discussion is based, primarily, on the data collected from the Felix No. 1 wells WS-10, WS-12, and WS-14.

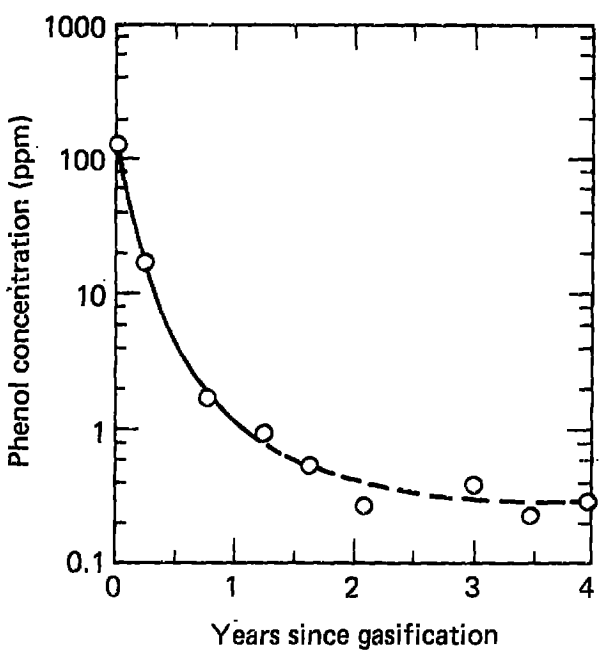


**FIG. 35. Decrease in phenol concentrations in groundwater near the edge of the Hoe Creek No. 1 cavity as a function of time. Data were obtained from a well located about 2 ft outside the cavity.**

In general, the concentrations of organic compounds are significantly larger in the Felix No. 1 Coal than in Felix No. 2, and the changes in the concentrations, as a function of time, are also quite different. An example is shown in Fig. 36, involving phenol concentrations in WS-10 and WS-12. One year after gasification, water from WS-10 had 37 ppm phenols, which is almost 30 times larger than the phenol concentration in WS-5 (Felix No. 2). The two wells are about the same distance from the cavity. The rapid increase of phenols in WS-12 (more than 100 ft from the cavity), a year after the Hoe Creek No. 2 experiment, is also interesting and surprising, since the hydraulic head measurements (Fig. 26) suggest that the water in the Felix No. 1 Coal aquifer probably flows very slowly. A possible explanation involves the deposition of pyrolysis products near WS-12 during gasification.

On the basis of the Felix No. 1 water-quality measurements, we have considered an alternative mechanism for the introduction of organic contaminants into the surrounding coal during gasification. Pyrolysis occurs within the walls of the cavity as a result of cavity heat, but, in general, the products formed in this manner are expected to be forced back into the cavity by steam generation in the cavity walls. However, the hot product gases (~1000°C) that escape into the coal must also produce pyrolysis reactions along the surfaces of the cracks through which they escape. The resulting volatile pyrolysis products will be swept further into the coal by the escaping gases. As gasification continues, and especially if some of the cracks in the coal are comparatively large (as some Hoe Creek evidence suggests), these pyrolysis products will be "distilled" farther out in the surrounding coal, and deposited on the surface along the cracks. Furthermore, since the hydrostatic pressure is lower in the overlying Felix No. 1 Coal than in Felix No. 2, the product gas within the cavity, whose pressure has been used to restrict groundwater entry and is approximately uniform throughout the cavity, will escape preferentially into the upper coal seam (Fig. 37). In other words, if the cavity pressure is adjusted to exclude groundwater from Felix No. 2, it may be sufficient to promote excess gas leakage into the upper coal. As a result of the difference in gas leakage rates, more volatile contaminants will be dispersed into—or, perhaps, produced in—the upper (Felix

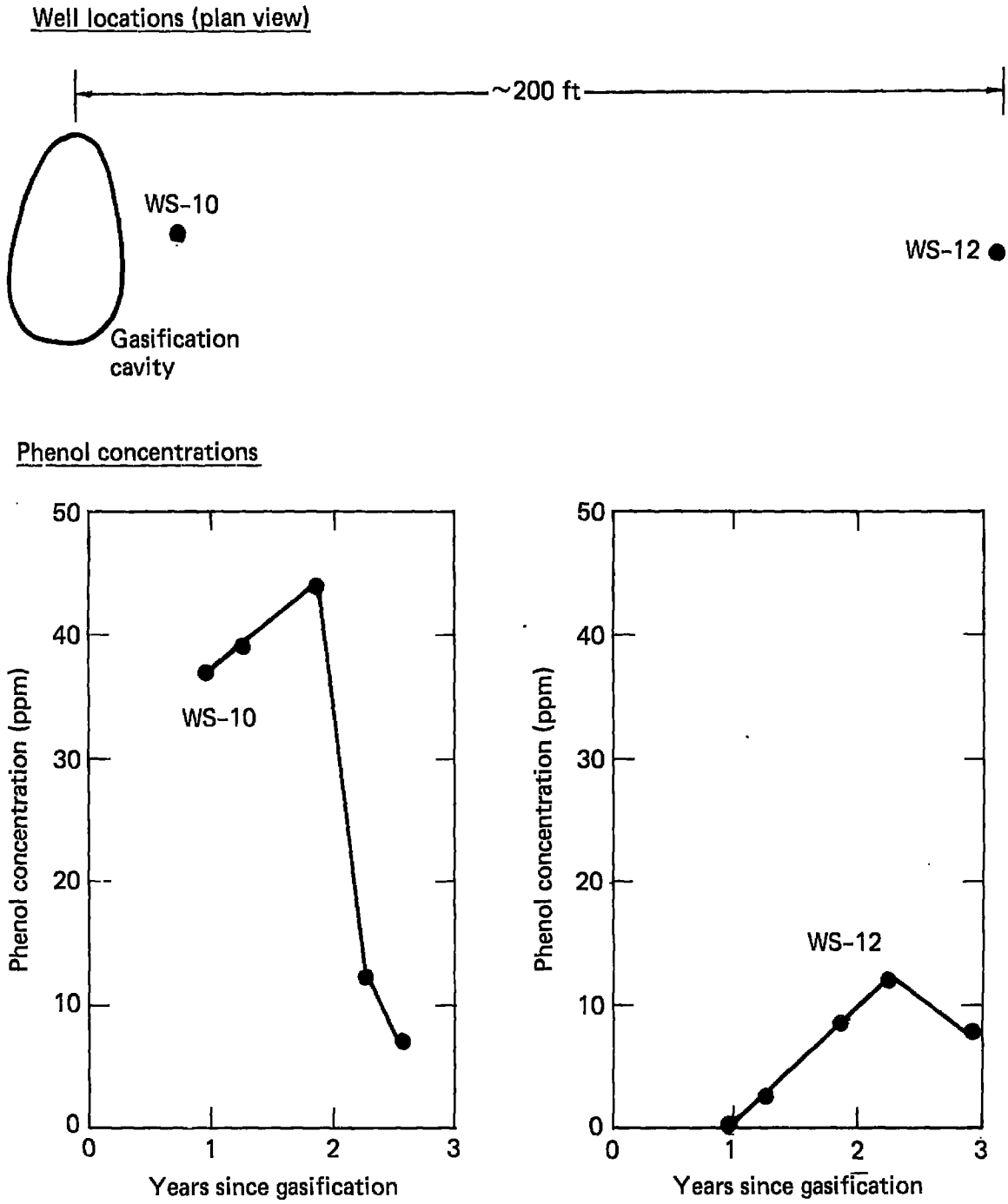


**FIG. 36. Change in phenol concentrations in the Felix No. 1 Coal aquifer as a function of time since the Hoe Creek No. 2 experiment.**

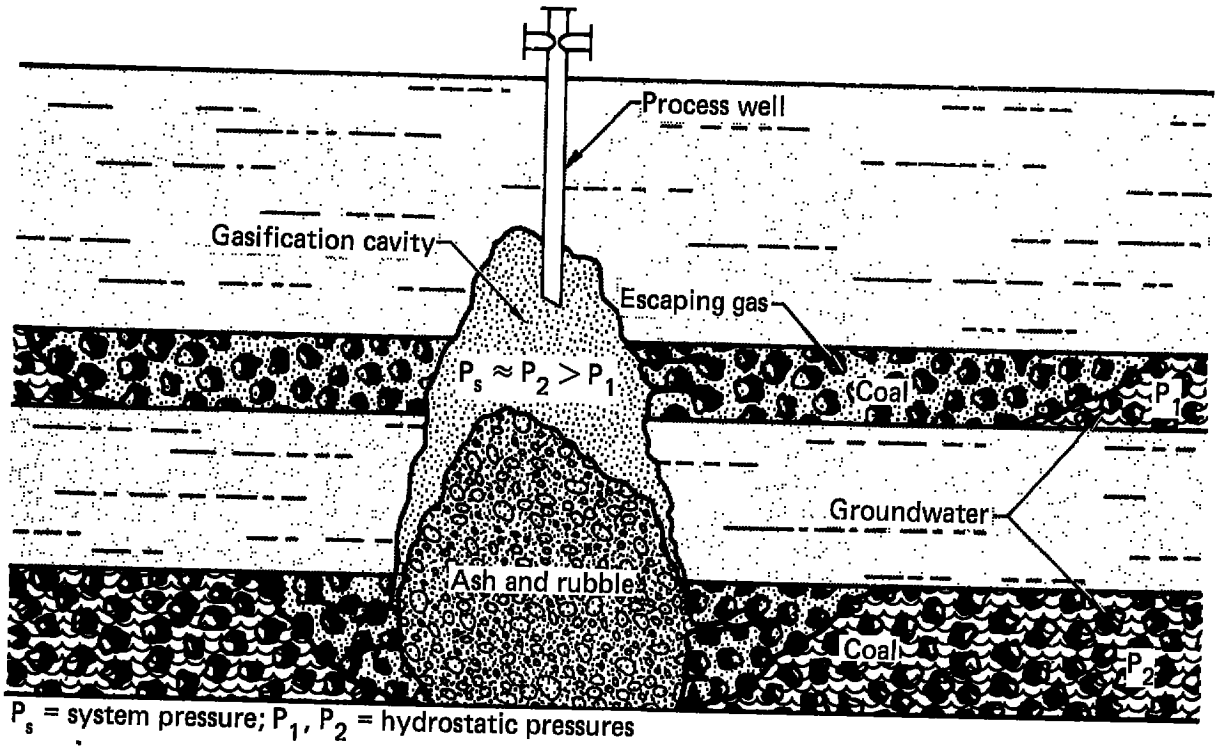


**FIG. 37. Schematic representation of the cavity and surrounding coal during gasification. Preferential penetration of hot product gases into the upper coal aquifer may cause increased production of pyrolysis products (potential groundwater contaminants) in the upper aquifer.**

No. 1) coal. It should be noted that differences in the groundwater flow in the two aquifers will also cause differences in the water quality of the two coal aquifers.

If the hypothesis concerning preferential gas leakage into the upper coal is correct, and the effect is significant, its importance may lie in the fact that a thick coal seam would represent a situation that is in some respects similar to the two coal seams gasified at Hoe Creek. That is, organic contaminants might be dispersed excessively into the top portion of the coal if cavity gas pressure is kept high enough to adequately restrict groundwater influx.

It is important to examine these proposed mechanisms for contaminant production and dispersal, since they are potentially subject to partial control. For example, the use of dewatering wells to control water influx might permit a lower system pressure, with the result that a smaller amount of product gas would escape into the coal, and the organic contaminants might be deposited closer to the cavity.

As we mentioned before, the hydraulic head in the Felix No. 1 Coal is almost the same as that inside the cavity. We therefore expect that cavity contaminants (the ash leachate) will be transported more slowly from the cavity into Felix No. 1 than into Felix No. 2. A comparison of the transport of boron species from the cavity to WS-5 (Felix No. 2) and WS-10 (Felix No. 1) is shown in Fig. 38. We do not believe that significant amounts of the contaminants that result from ash leaching have reached well WS-12. But other pyrolysis products have shown changes similar to the phenol changes in wells WS-10 and WS-12. Plots of changes in the concentrations of ammonium, cyanide, and dissolved organic carbon in WS-10 and WS-12 are shown in Figs. 39–41. At present, we have no definite evidence to show that the water in well WS-14 (Felix No. 1, 40 ft from well A) is contaminated with organic pyrolysis products, but we do see an increase in carbon dioxide (200 ppm vs a baseline value of 60 ppm). We have mentioned the decreases of sulfate in the groundwater inside the

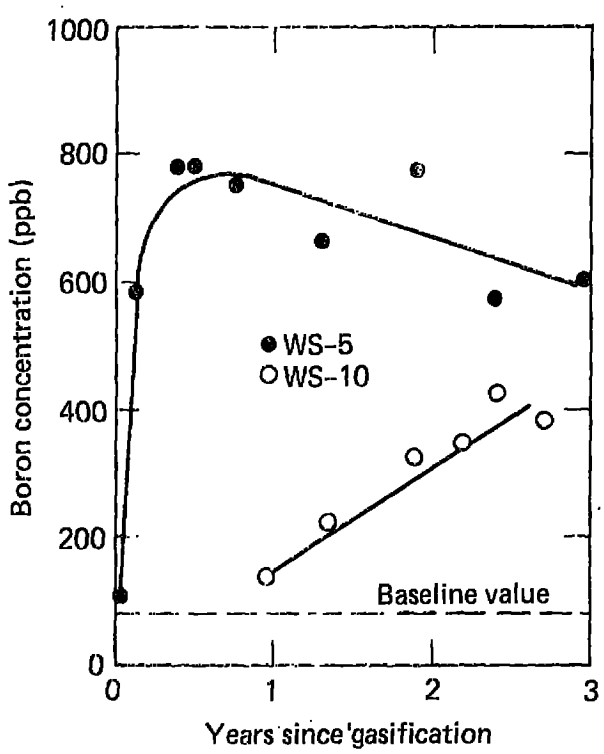


FIG. 38. Comparison of the change in boron concentration with time in WS-5 (Felix No. 2 Coal aquifer) and WS-10 (Felix No. 1).

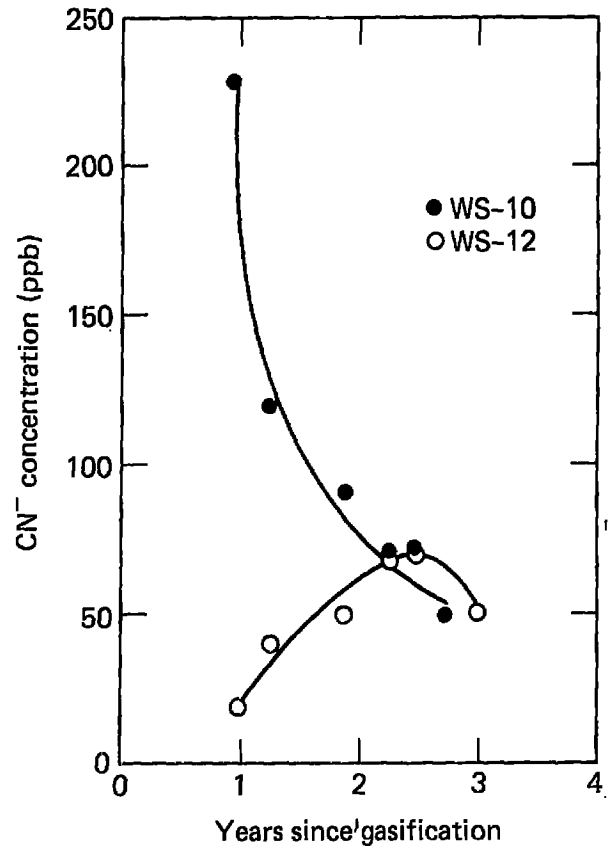


FIG. 40. Comparison of the change in cyanide concentration with time in WS-10 and WS-12.

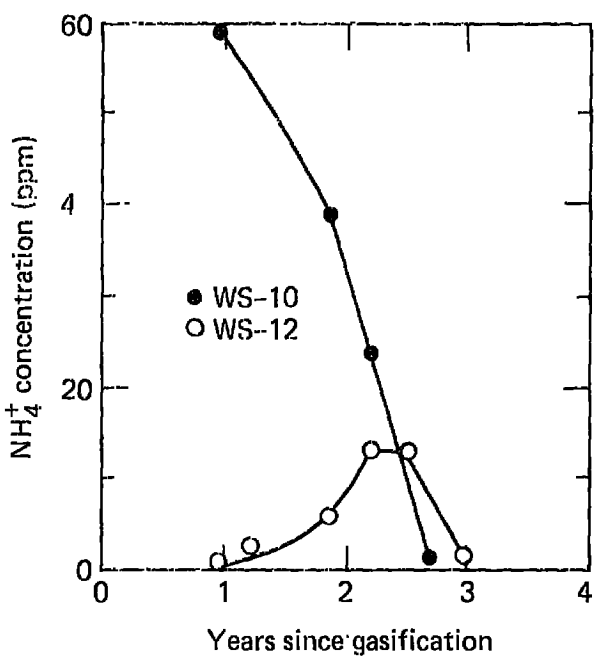


FIG. 39. Comparison of the change in ammonium concentration with time in WS-10 (55 ft from injection well A) and WS-12 (163 ft from well A).

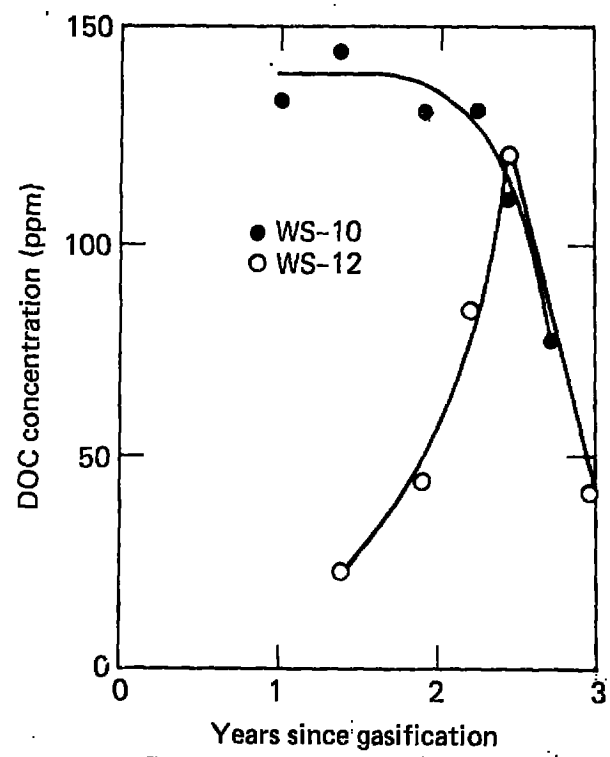


FIG. 41. Comparison of the change in dissolved organic carbon with time in WS-10 and WS-12.

cavity and in the Felix No. 2 Coal aquifer. The reduction of sulfate in the Felix No. 1 Coal aquifer is much more drastic, as shown in Fig. 42.

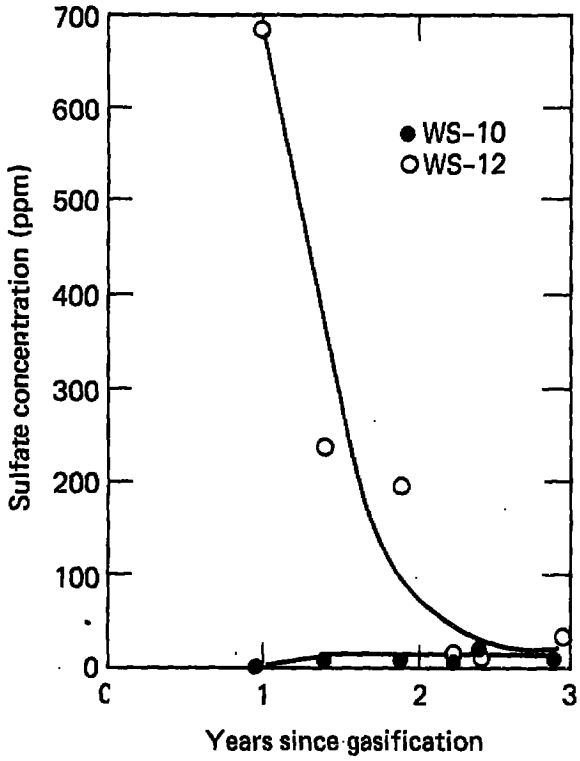


**FIG. 42. Comparison of the change in sulfate concentration with time in WS-10 (~20 ft from the cavity) and WS-12 (~130 ft from the cavity). Both wells are in the Felix No. 1 Coal aquifer. Baseline value is about 900 ppm.**

**The Sand Aquifer**

We have completed six water-sampling wells in the overlying sand aquifer near the Hoe Creek No. 2 site (Fig. 27 and Table 4). Some data have been obtained from three of these wells (WS-15, -16, -17), but no data are as yet available from the remaining three, which were completed recently.

In general, the water from the sand aquifer shows a lower concentration of pyrolysis products than the Felix No. 1 water. Since we have, as yet, only limited data, we are not able to discuss changes in contaminant concentrations. We list the measured contaminant species and parameters in Table 5. Well WS-17 is of particular interest because it appears to be very close to the cavity; its water temperature is the same as that inside the cavity. We have noted that the ammonium and boron concentrations in WS-17 are much lower than those inside the cavity (0.24 ppm vs 26 ppm for ammonium, and 0.14 ppm vs 1.6 ppm for boron). The other two sand aquifer wells still have boron concentrations at the baseline level.

The lower levels of contamination within the sand aquifer are consistent with our hypothesis that the hot product gases escaping into the coal seam pyrolyze the coal and may make a significant contribution to the residual organic contaminants. Hot gases escaping into a sand aquifer would not, of course, produce additional pyrolysis products.

—F. T. Wang and S. W. Mead

# REFERENCES


1. E. R. G. Eckert and R. M. Drake, *Heat and Mass Transfer* (McGraw-Hill, New York, 1959).
2. W. M. Kays, *Convective Heat and Mass Transfer* (McGraw-Hill, New York, 1966).
3. For a more detailed report on burn cavity growth in Hoe Creek No. 3, see R. W. Hill, *Burn Cavity Growth During the Hoe Creek No. 3 Underground Coal Gasification Experiment*, Lawrence Livermore National Laboratory, Livermore, Calif., UCRL-85173 (1981).



WC/kt

U. S. Government Printing Office: 1981/5–789-002/6576